Formation of amphitheater-headed valleys by waterfall erosion after large-scale slumping on Hawai‘i

Michael P. Lamb†
Department of Earth and Planetary Science, University of California, Berkeley, California 94720-4767, USA

Alan D. Howard
Department of Environmental Sciences, University of Virginia, Charlottesville, Virginia 22904-4123, USA

William E. Dietrich, J. Taylor Perron
Department of Earth and Planetary Science, University of California, Berkeley, California 94720-4767, USA

ABSTRACT

Amphitheater-headed valleys are common on the surfaces of Earth and Mars. The abrupt terminations of these valleys at their headwalls have been used extensively to argue for valley erosion from springs (i.e., seepage erosion or groundwater sapping) rather than surface runoff. This interpretation has significant implications for Martian hydrology and the associated prospects for life. A connection between channel form and the erosion processes induced by groundwater, however, has not been demonstrated in resistant rock. Perhaps the most widely cited terrestrial analogs for Martian amphitheater-headed valleys in basalt are the spectacular canyons of Kohala, Hawai‘i. Here we present new field observations and topographic analyses of the amphitheater-headed Kohala valleys. We found no evidence for intensively weathered rocks or alcoves around springs at valley headwalls. Instead, valley-head erosion appears to be dominated by waterfall plunge pools. Stream flow from peak annual precipitation events exceeds spring discharge by more than an order of magnitude, and such flow is responsible for evacuation of the coarse sediment that lines the streams. Bathymetric surveys along the Kohala coast have revealed a large submarine landslide, the Pololū Slump, directly offshore of the Kohala valleys. We propose that the headscarp of this massive landslide is expressed as the present-day ~400 m Kohala sea cliffs. As dominant streams poured over this headscarp as waterfalls, vertical plunge pool erosion and undercutting caused upstream propagation of knickpoints, eventually producing amphitheater-headed valleys. Island subsidence rates and the ages of volcanic eruptions and submarine terraces indicate that the average rate of valley headwall advance is as high as 60 mm/yr. We propose a simple expression for upslope headwall propagation by vertical waterfall erosion based on abrasion by impacting sediment particles in plunge pools. This model indicates that headwall propagation depends nonlinearly on the sediment flux passing over the waterfall and linearly on the ratio of kinetic versus potential energy of sediment impacts. After the Pololū Slump, many streams did not form upslope-propagating waterfalls because they had smaller discharges due to a radial drainage pattern and fault-bounded drainage divides, which prevented runoff from the wetter summit of the volcano. A threshold for headwall propagation due to sediment supply or sediment-transport capacity is consistent with the model. Island subsidence following valley formation has resulted in alluviation of the valley floors, which has created the observed U-shaped valley cross sections. Our interpretation implies that surface runoff can carve amphitheater-headed valleys and that seepage erosion cannot be inferred based solely on valley form on Earth, Mars, or other planets.

Keywords: amphitheater, sapping, seepage, Hawai‘i, knickpoint, plunge pool, waterfall.

INTRODUCTION

Spectacular amphitheater-headed valleys line the coastlines of Kaua‘i, O‘ahu, Moloka‘i, Maui, and Hawai‘i (Fig. 1). The origin of the steep, stubby (i.e., box-shaped planform geometry) headwalls and flat floors of these valleys has been debated for more than 80 years (Hinds, 1925; Davis, 1928; Wentworth, 1928; Stearns and Vaksvik, 1935; Cotton, 1943; Stearns and Macdonald, 1946; White, 1949; Macdonald et al., 1983; Stearns, 1985; Kochel and Piper, 1986; Kochel and Baker, 1990; Howard et al., 1994; Craddock and Howard, 2002; Lamb et al., 2006). The leading hypothesis has been that seepage-induced chemical weathering at the intersection between the water table and streambed leads to development of a knickpoint (Wentworth, 1928; Stearns and Macdonald, 1946; White, 1949; Kochel and Piper, 1986; Kochel and Baker, 1990). Seepage erosion at the base of the knickpoint is proposed to cause undercutting (i.e., sapping), collapse, and subsequent upstream propagation of the knickpoint, eventually forming the steep valley headwall. Since the 1980s much attention has been given to the Hawaiian valleys because of their apparent similarity to Martian amphitheater-headed valleys in morphology and potentially in lithology (i.e., basalt). Small physical experiments have shown that amphitheater-headed valleys with flat floors can result from seepage erosion in loose sand (e.g., Howard and McLane, 1988). Similarity in form has been used to infer process, such that the connection between seepage erosion and amphitheater-headed valleys in sand has been used to argue for seepage erosion on Hawai‘i and, by analogy, Mars (Kochel and Piper, 1986; Kochel and Baker, 1990; Gulick, 2001). A seepage origin of Martian valleys would be significant because it could indicate an early Mars that did not support rainfall (Pieri, 1976; Carr and Clow, 1981; Squyres, 1989; Malin and Carr, 1999) or that precipitation infiltrated to cause seeps without appreciable direct runoff (e.g., Grant, 2000).

The seepage erosion hypothesis for Hawai‘i has not been without criticism. While springs have been found in some Hawaiian valleys, they are often high up the valley walls where they seem to drain perched aquifers associated

†E-mail: mpl@berkeley.edu.

GSA Bulletin; July/August 2007; v. 119; no. 7/8; p. 805–822; doi: 10.1130/B25986.1; 11 figures; 2 tables.

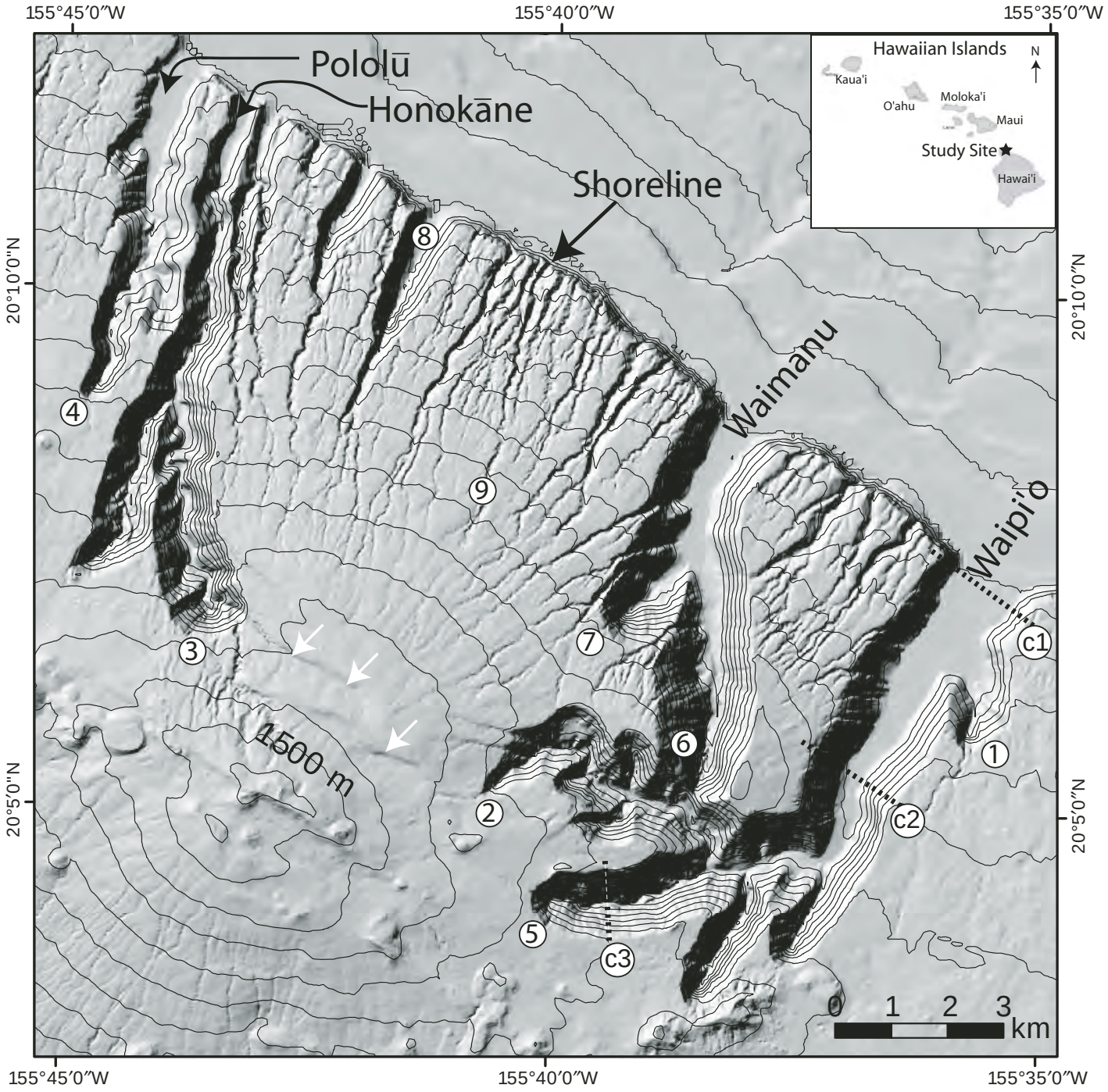

Figure 1. 10 m shaded relief and topographic contour map of northeast side of Kohala Volcano. Contour interval is 100 m. The 1500 m contour is labeled. Present-day sea level is at 0 m. The four large Kohala amphitheater-headed valleys are named on the figure. Longitudinal profiles for valleys numbered 1–9 are given in Figure 6, and associated data are given in Table 1. Dotted lines across Waipi'o Valley are cross sections (c1–c3) given in Figure 7. Faults that funnel high-elevation drainage to the amphitheater-headed valleys near the volcano summit are indicated by white arrows. Data are from U.S. Geological Survey (7.5′ quadrangles), Monterey Bay Aquarium Research Institute, and U.S. Army Corps of Engineers Laser Imaging Detection and Ranging (LIDAR) (datum: NAD 83, projection: UTM zone 5). The inset figure in the upper right corner shows the location of the study site in the Hawaiian Islands.

with less-permeable ash layers (Stearns and Macdonald, 1946). To our knowledge, there are no published field observations documenting weathering or erosion associated with Hawaiian springs. Indeed, well-developed alcoves, secondary porosity, or obviously weathered rocks are rare (Howard et al., 1994). Furthermore, several springs issue from the sea cliffs along the present-day shoreline and do not have canyons or alcoves associated with them (Stearns and Macdonald, 1946). In loose sediment (e.g., Howard and McLane, 1988; Uchupi and Oldale, 1994; Schumm et al., 1995) or weakly cemented sedimentary rocks (e.g., Laity and Malin, 1985; Howard and Kochel, 1988; Nash, 1996), seepage erosion is a plausible hypothesis for canyon formation (Lamb et al., 2006). In resistant rock like basalt, however, seepage must first weather the rock to transportable-sized particles before erosion can occur (Dunne, 1990; Dietrich and Dunne, 1993). If seepage flow cannot transport collapsed debris away from the valley headwall, then talus will buttress the headwall and prevent retreat.

Here we present an alternative model for the formation of the Hawaiian amphitheater-headed valleys. The Hawaiian amphitheater-headed valleys typically form on the wet sides of the islands and often have spectacular waterfalls at their headwalls. Based on observations of well-developed plunge pools, we propose that waterfalls have been the dominant erosive agent causing headwall retreat, rather than seepage erosion. This idea is not new; many workers have suggested that waterfall processes are important for headwall erosion in Hawai'i (Stearns and Vaksvik, 1935; Macdonald et al., 1983; Howard et al., 1994; Craddock and Howard, 2002). We expand on previous work using new field observations and topographic analyses to hypothesize the origin of large knickpoints from massive landslides. We calculate the rates of knickpoint propagation using recently acquired bathymetric maps coupled with age determinations of Hawaiian basalts and marine terraces. Lastly, a simple mechanistic rule is proposed for waterfall plunge-pool erosion and headwall propagation following recent developments in bedrock-erosion theory (e.g., Sklar and Dietrich, 2004). Our study is focused on the largest, youngest, and perhaps most impressive set of these valleys: Waipi'o, Waimanu, Honokāne, and Pololū Valleys on the northeast side of Kohala Volcano on the island of Hawai'i (Fig. 1).

CONSTRUCTION AND SUBSIDENCE OF KOHALA VOLCANO

Kohala Volcano, on the island of Hawai'i, began subaerially erupting the basaltic Pololū volcanic rocks at ca. 700 ka, and this continued to ca. 250 ka (Dalrymple, 1971; McDougall and Swanson, 1972; Wolfe and Morris, 1996). During this period of volcanism, the Kohala shield was constructed, and a distinct break in slope was formed at paleo–sea level because subaqueously chilled lava solidifies at a steeper slope than subaerial lava (Moore and Clague, 1992). This break in slope is referred to here as a "volcanic terrace" following Moore and Clague (1992). Near the end of the shield-building stage, the volcano experienced a relative sea-level rise due to isostatic subsidence as indicated by several drowned coral reefs off the west flank of Kohala (Fig. 2). The volcanic terrace is now ~1000 m below present-day sea level (Moore and Clague, 1992) (Fig. 2), indicating 1000 m of relative sea-level rise since the terrace was formed. Subsidence has occurred at roughly a steady rate of 2.6 mm/yr based on radiometric ages of drowned coral reefs (Fig. 2) (Moore and Fornari, 1984; Szabo and Moore, 1986; Ludwig et al., 1991). We estimate that the volcanic terrace formed ca. 385 ka by dividing the subsidence distance of 1000 m by the mean subsidence rate of 2.6 mm/yr. A drowned reef at 950 m below present-day sea level yielded radiometric ages of 248–314 ka (Ludwig et al., 1991; Jones, 1995), which is consistent with this estimate. It should be noted that scatter about the mean subsidence rate exists and might be due to erosion of the reefs, differential subsidence, landsliding, or diagenetic effects that alter the dating technique (Moore and Clague, 1992; Ludwig et al., 1991). After the shield-building stage, the Hawi volcanic series erupted, and it unconformably overlies the Pololū volcanic series (Fig. 3). The Hawi volcanic series ranges in age from 230 to 120 ka (McDougall and Swanson, 1972; Wolfe and Morris, 1996).

During subsidence of Kohala Volcano, a second large volcanic terrace from the younger Mauna Kea Volcano was formed along the northeast shoreline of Kohala and has since subsided ~450 m below present-day sea level (Fig. 2). The age of this terrace must be within the range in ages of Mauna Kea volcanic rocks from 250 ka to 65 ka (Wolfe and Morris, 1996). The terrace must also be older than a drowned coral reef at –360 m that has a radiometric age of ca. 120 ka (Moore and Fornari, 1984; Szabo and Moore, 1986; Ludwig et al., 1991). We estimate that the Mauna Kea terrace formed ca. 173 ka (and therefore records the location of the paleoshoreline at this time) using the mean subsidence rate of 2.6 mm/yr (i.e., 450 m ÷ 2.6 mm/yr = 173 ka).

Gravel terraces on Kohala Volcano at altitudes as high as 300 m above present-day sea level indicated to Stearns and MacDonald (1946) that the island has undergone partial emergence, not continuous submergence. These deposits, however, have been reinterpreted as tsunami deposits associated with one of the many huge landslides of the Hawaiian Islands (McMurtry et al., 2004).

POLOLŪ SLUMP AND KOHALA SEA CLIFFS

A massive landslide, the Pololū Slump, occurred directly offshore of the Kohala amphitheater-headed valleys on the northeast flank of Kohala Volcano (Fig. 2). This landslide was ~20 km wide and traveled 130 km (Moore et al., 1989; Moore and Clague, 1992). The most obvious features of the slump are huge disorganized blocks below the 1000 m isobath (Fig. 2). Upslope of the blocks, there is a broad ~400 m bathymetric depression, which likely represents the slump scar or a down-dropped block related to the slump (Smith et al., 2002). It is difficult to reconstruct the dimensions of the slump scar due to postslumping carbonate and siliciclastic sedimentation. Further complicating the bathymetry are several submarine canyons, which cut through the bathymetric depression (Figs. 1 and 3). These canyons have the greatest relief near their heads, and they become shallower downstream, where they are indistinct at a depth of ~900 m. The canyons are cut into a carbonate platform (Clague et al., 1998) and likely formed from submarine processes, such as turbidity currents. Several of the canyons end abruptly in amphitheater heads, which led to the interpretation that they were formed by dissolution of the carbonate platform by freshwater seepage (Clague et al., 1998).

The prominent (up to 450 m high) Kohala sea cliffs (Fig. 4) are directly upslope of the slump scar. The Kohala cliffs are anomalous in that neighboring sea cliffs are consistently only 20–50 m high (Fig. 4). The shoreline of Hawai'i generally follows the topographic contours of the volcanoes, and at the scale of tens to hundreds of meters, it is relatively jagged in planform. In the region of the high cliffs, the shoreline is remarkably straight in planform. Since the volcano is dome shaped, the straight shoreline cuts across topographic contours, resulting in the greatest relief in the middle of the cliffs (Fig. 4). The Kohala cliffs also are abruptly inset ~2.5 km from the adjacent sections of the Hawaiian shoreline (Fig. 3). These observations suggest that the Kohala sea cliffs are the bounding headwall of the Pololū Slump (Wolfe and Morris, 1996). The near vertical failure plane would explain why the cliffs are anomalously high, straight in planform, inset significantly from the rest of the shoreline, and cut across topographic

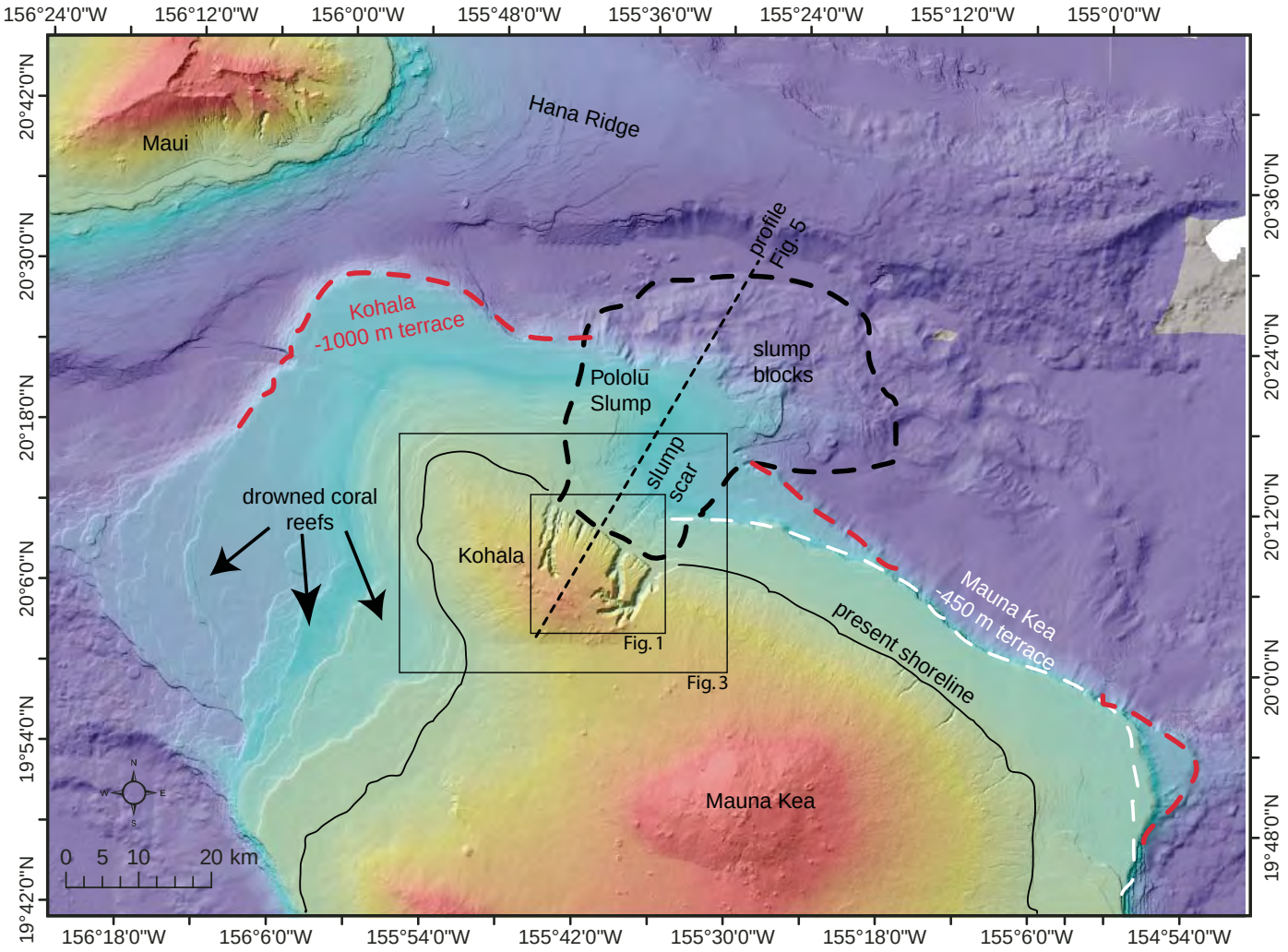

Figure 2. Shaded relief map of the northern half of Hawai'i and associated bathymetry. Data resolution varies among different data sets. Hot and cold colors correspond to high and low elevations, respectively. The following interpretations are following Smith et al. (2002): the Pololū Slump is outlined with a black dashed line; Mauna Kea terrace at –450 m (shoreline at the end of the shield-building stage) is marked by a white dashed line; the Kohala terrace at –1000 m is marked by a red dashed line. The present shoreline is outlined with a thin solid black line. See text for details. The thin black dashed line is the location of the slump profile shown in Figure 5. The two black boxes indicate the locations of the maps shown in Figures 1 and 3. Data sources include U.S. Geological Survey, Monterey Bay Aquarium Research Institute, U.S. Army Corps of Engineers Laser Imaging Detection and Ranging (LIDAR), National Geophysical Data Center (National Oceanic and Atmospheric Administration), and Japan Marine Science and Technology Center.

contours. Figure 5 shows a longitudinal profile from the summit of Kohala Volcano through the Pololū Slump and a hypothetical illustration of a failure plane.

Stearns and Macdonald (1946) argued that the Kohala sea cliffs are anomalously high because they are composed of older and weaker basalt and therefore have experienced greater wave erosion. It is true that southeast of Waipi'o Valley the shoreline is composed of younger Mauna Kea flows. However, most of the shoreline northwest of Pololū Valley is composed of the same Pololū volcanic series as the Kohala cliffs (Fig. 3). Wave erosion might still explain the Kohala cliffs if wave attack was somehow focused in this region. This, however, seems unlikely because the Kohala cliffs are of roughly the same trend as the neighboring cliffs. Furthermore, wave erosion cannot easily account for the abruptly straight coastline that crosscuts topographic contours.

Moore et al. (1989) suggested that the headwall of the Pololū Slump is near the summit of Kohala Volcano where several extensional faults, akin to pull-apart basins, have been mapped (Stearns and Macdonald, 1946) (indicated by white arrows on Fig. 1). In such a scenario, Waipi'o and Pololū Valleys might follow faults that laterally bound the slump. Waipi'o and Honokāne Valleys do appear to follow these faults near their heads (Fig. 1). Smith et al. (2002) argued, however, that the surface of the volcano laterally bounded by Waipi'o and Pololū Valleys is continuous with the rest of the volcano summit, indicating little displacement. The volcano flank is actually slightly steeper in this region as compared to the neighboring slopes, which is not consistent with slumping. The faults near the summit of Kohala probably resulted from an ancient caldera (Stearns and Macdonald, 1946), or radial rift arms that accommodated hanging displacement as the Kohala rift zone extended

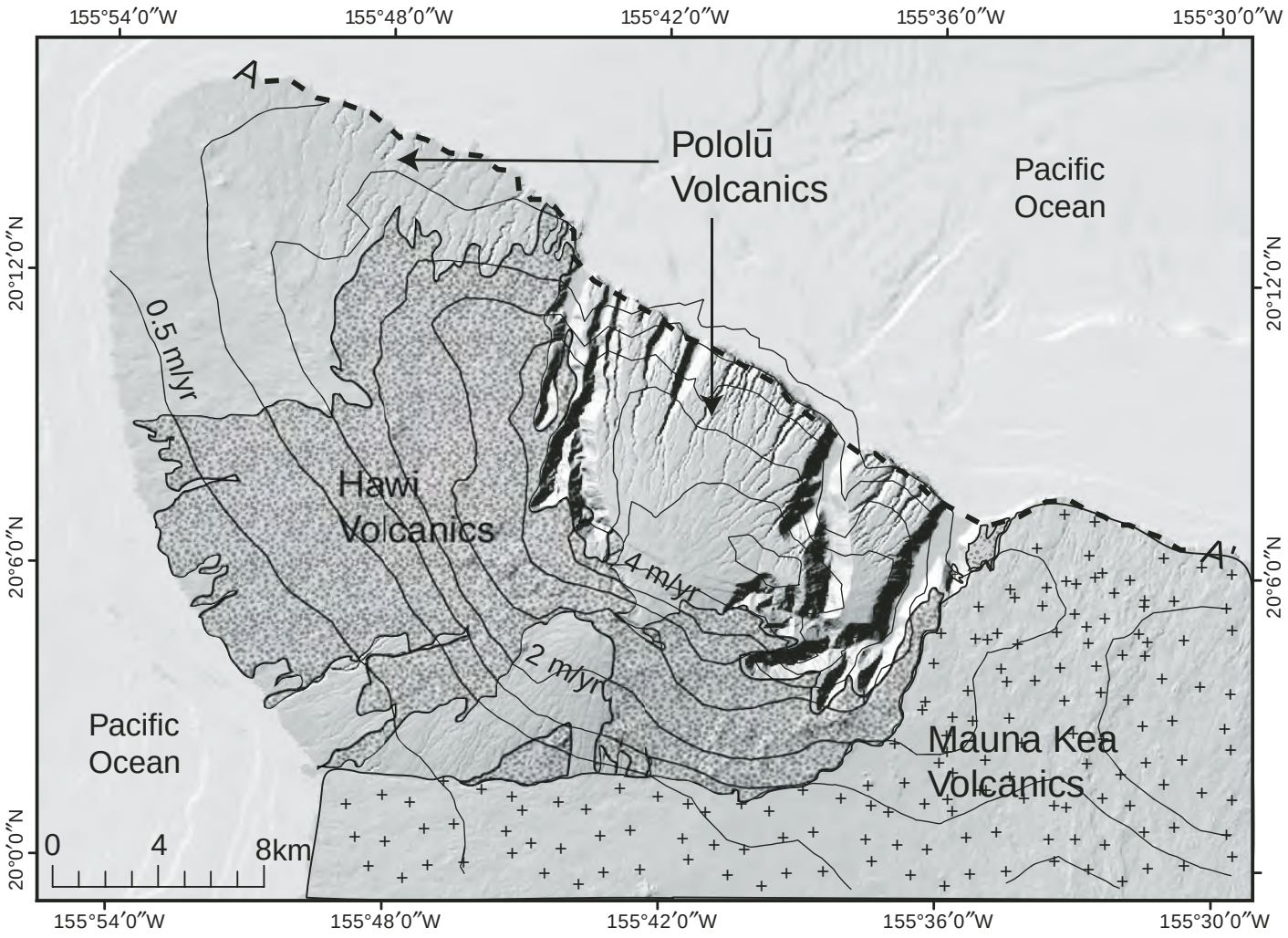

Figure 3. Shaded relief map of Kohala Volcano with volcanic units outlined following Wolfe et al. (1996). Note that the Pololū volcanic series is not patterned. Coastal profile A–A′ is shown in Figure 4. Contour map of average annual precipitation (1961–1990) is shown, with a contour interval of 0.5 m/yr, from PRISM climate model (Spatial Climate Analysis Service, Oregon State University, http://www.ocs.oregonstate.edu/prism/, created 4 February 2004). Note that orographic effects cause rainfall to exceed 4 m/yr near the heads of the amphitheater-headed valleys. See Figure 2 for topographic data sources.

(Smith et al., 2002). A few of these faults cross-cut both the Pololū and Hawi volcanic series. The majority of Hawi flows, however, appear to have been diverted to the northwest and southeast by the graben, which suggests that most of the displacement predates the Hawi volcanic series (Stearns, 1985).

The Pololū Slump, like other large Hawaiian landslides, likely occurred when the volcano was close to its maximum size (ca. 385 ka) and seismic and volcanic activity was high (Moore et al., 1989, 1994; Moore and Clague, 1992). Since the −1000 m terrace is only slightly disturbed in the region of the Pololū Slump (Fig. 2), Moore et al. (1989) hypothesized that the slump occurred prior to or during the formation of the −1000 m terrace. An alternate explanation is that the slump postdates the formation of the terrace and that the −1000 m isobath was not significantly disturbed because there was little displacement in this region, e.g., if the slump was rotational (Fig. 5). The latter interpretation is also consistent with the observation that the −1000 m isobath is ~5 km seaward in the region of the Pololū Slump as compared to the surrounding area (Figs. 2 and 5). Furthermore, the slump is composed of Pololū volcanic rocks and therefore is probably younger than 250 ka. In either scenario, the slump scar is overlain by the −450 m Mauna Kea terrace (Fig. 2), which restricts the slump to an age older than ca. 173 ka. If the faults near Kohala summit were caused by the slump, then the slump must be older than the eruption of Hawi volcanic series ca. 230 ka. These observations suggest that the slump occurred between 385 ka and 173 ka, and perhaps between 250 ka and 230 ka.

KOHALA AMPHITHEATER-HEADED VALLEYS

While streams have barely cut into the drier western slopes of Kohala Volcano, the amphitheater-headed valleys to the east are typically 300–750 m deep and terminate abruptly in steep headwalls (Fig. 1). These valleys have stubby heads (U-shaped in planform), which led to the "amphitheater" designation (Hinds, 1925). In order to analyze the Kohala valleys, we constructed longitudinal profiles for nine valleys that are typical of the range of valley morphologies

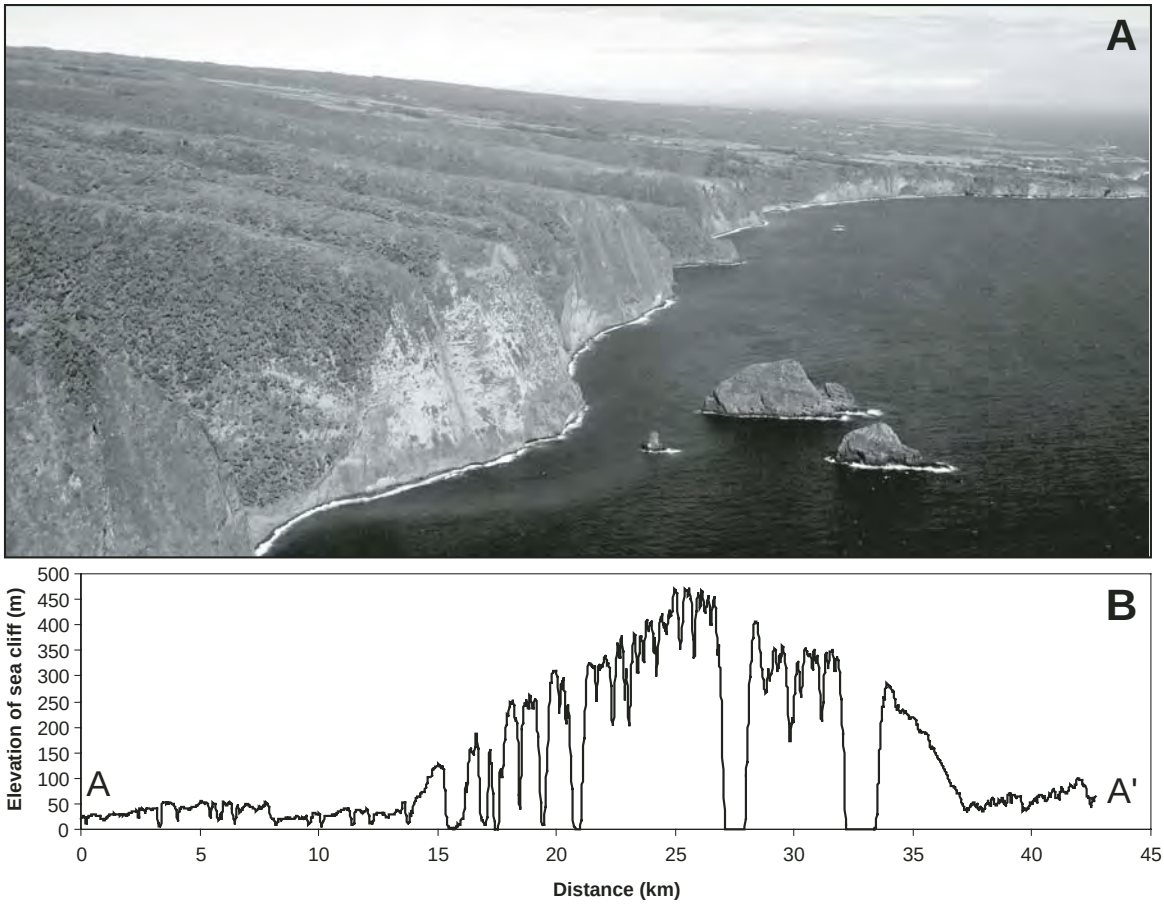

Figure 4. Kohala sea cliffs. (A) Photograph of Kohala sea cliffs. The sea cliff relief is approximately 400 m, for scale. (B) Topographic profile of sea-cliff elevation above present-day sea level extracted from 10 m digital elevation model (U.S. Geological Survey). Location of profile is shown as A–A′ on Figure 3. Note that in the region of the amphitheater-headed valleys, the sea cliffs are approximately an order of magnitude greater in elevation than neighboring cliffs. The mouths of Waimanu and Waipi'o Valleys are at ~28 and 33 km, respectively.

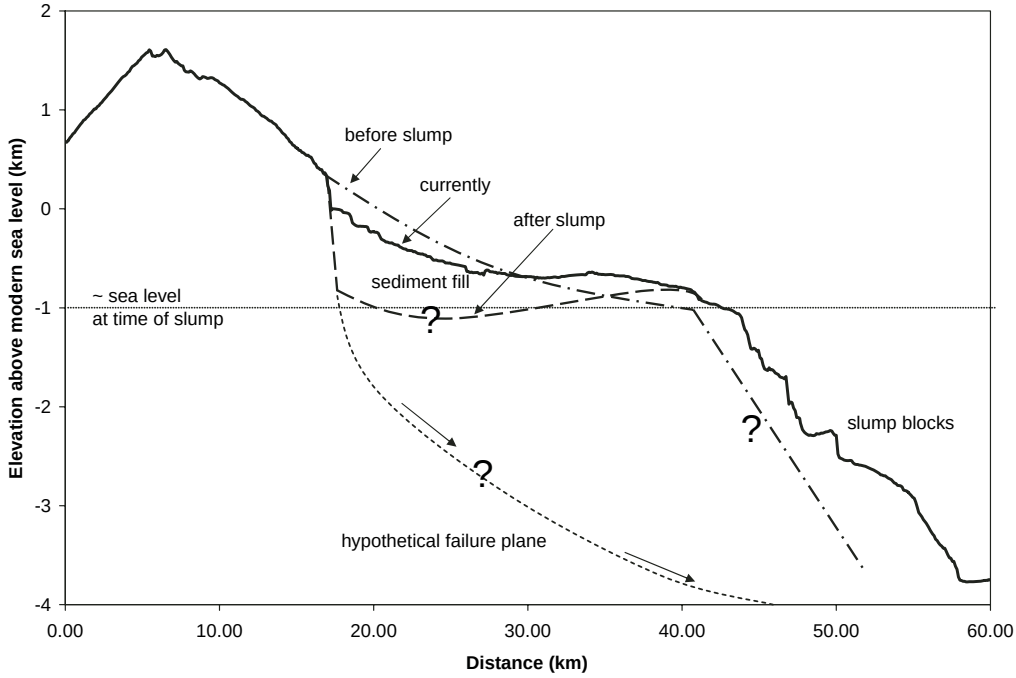

Figure 5. Topographic profile from Kohala Volcano over the Pololū Slump. Profile location is shown in Figure 2. All dashed lines are untested interpretations of the topography before and immediately after the Pololū Slump. Note that sea level at the time of the slump was probably ~1000 m lower than at present. The headscarp of the slump (expressed as the present-day sea cliffs) might have had 600–700 m of additional relief at the time of the slump, as indicated by the submergence of the valleys. Since that time, hundreds of meters of sediment have been deposited within the slump scar.

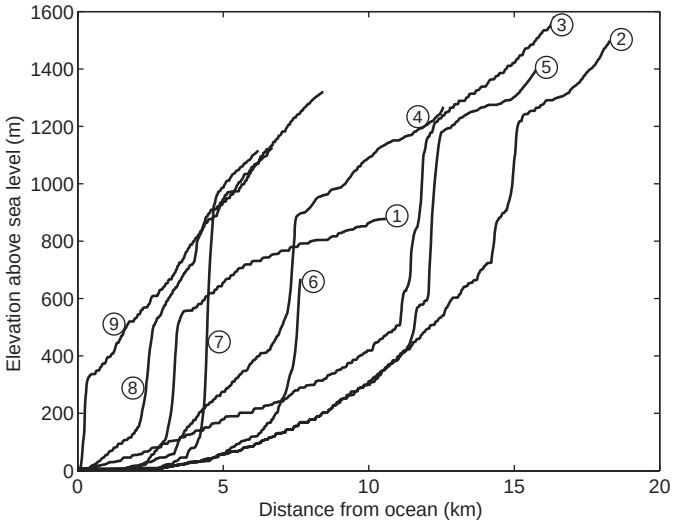

Figure 6. Longitudinal profiles from amphitheater-headed valleys (1–7), an intermediate valley (8), and a hanging valley (9). Profile 9 is representative of many valleys that are hanging at the sea cliffs, which are not shown here to avoid redundancy. The geographic locations of the valleys are shown in Figure 1. Profiles were generated following the steepest slope (D8) using a 10 m digital elevation model (U.S. Geological Survey). Much of the fine-scale variation is an artifact of the resolution of the grid. Depressions were artificially filled to generate the profiles. Profiles were chosen to represent the entire length of the drainage area from source to valley mouth. Note that lower portions of many of the amphitheater-headed valleys have subsided below present-day sea level and are filled with sediment.

in the region (Fig. 6). Valley numbers (1–9) are shown on Figure 1, and valley and stream characteristics are given in Table 1. Valleys 1–7 are amphitheater-headed valleys. Amphitheater-headed valleys have cut through the Kohala sea cliffs and have steep headwalls located several kilometers inland from the cliffs. The abrupt termination of the valleys at steep headwalls and the greater steepness of headwalls as compared to sidewalls suggests valley erosion by headwall propagation. This interpretation is further supported by stream piracy inferred from valley crosscutting relationships, as discussed below.

In contrast to the amphitheater-headed valleys, there are smaller valleys that have acutely pointed heads (i.e., gradually narrowing in planform) and longitudinal profiles that grade smoothly with the regional topographic slope (e.g., valley 9). These smaller valleys run alongside of and often drain into the larger canyons or pour over the Kohala sea cliffs (Fig. 4A) and will therefore be referred to as hanging valleys. There are a few valleys intermediate in size between the smaller hanging valleys and the larger amphitheater-headed valleys (e.g., valley 8). Intermediate valleys have pointed heads in planform like the hanging valleys, but they widen and deepen significantly near their mouths similar to the amphitheater-headed valleys.

Most of the upstream portions of the amphitheater-headed valleys are V-shaped in cross section (Figs. 7, 8A, and 8C), in contrast to the U-shape called for in the seepage-erosion model (Kochel and Piper, 1986; Kochel and Baker, 1990). As an example, Figure 7 shows three topographic cross sections of Waipi‘o Valley, the locations of which are shown on Figure 1. We found that most valley sidewalls have slopes of ~50°, despite being different-sized valleys with varying drainage areas. Soil production, vegetation growth, and shallow landsliding are active processes and are likely important in maintaining the relatively constant valley-wall slopes (Wentworth, 1943; White, 1949; Scott and Street, 1976; Stearns, 1985). While V-shaped in cross section near their headwalls, amphitheater-headed valleys are flat-floored near their mouths (Figs. 7 and 8B). This is not a result of seepage erosion, but rather of sedimentation concurrent with island subsidence (Stearns and Macdonald, 1946). The depth to which the valleys have been carved below present-day sea level is not known, but estimates range from 100 m (Macdonald et al., 1983) to more than 400 m (Stearns, 1985). Linear extrapolation of the side slopes of Waipi‘o Valley (Fig. 7) results in a bedrock valley floor ~600–700 m below present-day sea level. This, however, is an upper estimate because the valley walls have probably retreated laterally following subsidence.

The amphitheater-valley headwalls often have several plunge pools that interrupt cascading waterfalls and appear to dominate

TABLE 1. CHARACTERISTICS OF KOHALA VALLEYS

Valley no.	Stream/valley name	Morphology	Average annual peak discharge (m^3/s)	Spring flow (m^3/s)	Migration distance (km)	Drainage area (km^2)
1	Hiilawe/Waipi‘o	Amphitheater	?	0.35	3.33	16.46
2	Kawainui & Kawaiki/Waipi‘o	Amphitheater	41.40	0.35–0.96	15.06	8.51
3	East Honokāne	Amphitheater	?	0.46–0.59	11.85	8.38
4	Pololū	Amphitheater	?	0	7.46	4.31
5	Alkahi/Waipi‘o	Amphitheater	12.47	?	12.15	3.92
6	Waimanu/Waimanu	Amphitheater	?	0.22–0.52	7.56	0.58
7	Waihilau/Waimanu	Amphitheater	?	0.22–0.52	4.41	1.54
8	Honopue	Intermediate	?	?	2.47	4.49
9	Waikaloa	Hanging	?	?	0.26	4.15

Note: Locations of valleys are shown on Figure 1, and longitudinal profiles are shown on Figure 6. Annual peak discharge is from U.S. Geological Survey (gauge 16720000, 16720300, 16725000) averaged over a 40 yr period. Spring flow measurements are from Stearns and MacDonald (1946) and Kochel and Piper (1986). Knickpoint migration distance was measured from the longitudinal profiles (Figure 6) as the distance from the present-day shoreline to the location of maximum slope, which typically corresponds to midway up the headwall for the amphitheater and intermediate valleys, and midway up the sea cliffs for the hanging valley (which is why valley 9 has a nonzero migration distance). Drainage area is the contributing area to the valley heads (waterfalls) for the amphitheater and intermediate valleys, and to the sea cliffs for the hanging valley. Note that the drainage areas to the valleys have changed in time due to upslope propagation of knickpoints and stream capture.

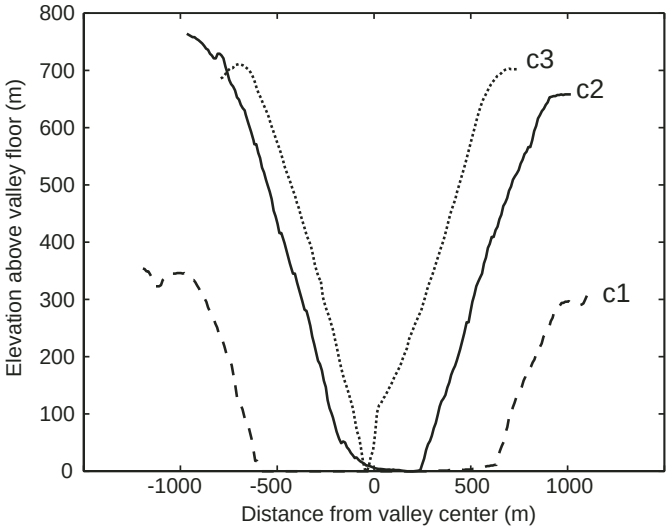

Figure 7. Cross sections of Waipi‘o Valley. Profiles were generated from a 10 m digital elevation model (U.S. Geological Survey). Profile locations are shown as dotted lines on Figure 1. These cross sections are typical of the other amphitheater-headed valleys—near their heads the valleys are V-shaped, while near their mouths the valleys are U-shaped due to relative sea-level rise and sedimentation. The true bedrock valley bottom at c1 might extend 600–700 m below present-day sea level based on linear extrapolation of the valley-wall slopes.

erosion of valley headwalls (Figs. 8C–8E). Howard et al. (1994) inferred that stepped waterfalls are vertically drilling into the rock through the impact of falling water and sediment. Figure 8D shows coarse sediment deposited within and next to plunge pools that must have been delivered by the waterfalls. In some cases, plunge-pool erosion also appears to be undercutting the headwall (Fig. 8E), possibly exploiting weaker beds in the layered volcanic rock. The locations of the plunge pools do not seem to correlate with any major discontinuities in rock strength (unlike classic models of waterfall erosion, e.g., Niagara Falls [Gilbert, 1907]). Instead, plunge pools are at different elevations and often in a series of steps along a single flow path. During high-precipitation events, tens of waterfalls can be active at a single valley head (personal commun. with local residents, 2004; Figs. 8C–8E).

Springs do exist in the Kohala valleys, as one would expect in any deeply incised canyon that intersects the water table. However, we have not observed weathered rock or overhangs associated with springs, which are expected indicators of seepage erosion (Lamb et al., 2006). Peak-annual surface flows exceed spring discharges by nearly two orders of magnitude (Table 1). Coarse debris that lines the streambeds must be transported away from valley headwalls for headwall propagation to occur. Spring discharges are presently incapable of transporting this material.

If valley formation occurred from upstream propagation of valley headwalls due to waterfall erosion, then one might expect there to be a correlation between headwall migration distance and stream discharge (e.g., Whipple and Tucker, 1999; Hayakawa and Matsukura, 2003; Bishop et al., 2005; Crosby and Whipple, 2006). Using the digital elevation data shown in Figure 1, we calculated the contributing drainage area to the dominant knickpoints in the valley profiles (i.e., the headwalls for the amphitheater and intermediate valleys, and the Kohala sea cliffs for the hanging valleys). Drainage area is used as a proxy for stream discharge because historic stream records are only available for two sites (Table 1). All of the intermediate and hanging valleys in the Kohala region have drainage areas less than 5 km^2. For example, valleys 8 and 9, which are two of the largest intermediate- and hanging-type valleys, have drainage areas of 4.49 and 4.15 km^2, respectively. In contrast, the amphitheater-headed Waipi‘o Valley (valley 2) and West Honokāne Valley (valley 3) have two of the largest drainage areas, ~8 km^2 each (Table 1). Valleys 2 and 3 also drain the very wet Kohala summit (Fig. 3), have what visually appears to be the most active plunge pools (Figs. 8C–8E), and have two of the longest headwall-propagation distances from the present-day sea cliffs of ~15 and 12 km, respectively (Table 1).

Several of the amphitheater-headed valleys, however, do not appear to follow a trend of increasing headwall migration distance with increasing drainage area. For example, Hiilawe Valley (valley 1) has the largest drainage area of any of the amphitheater valley heads, ~16 km^2, but its headwall is only ~3 km from the sea cliffs (Fig. 1). Part of the reason for this is that Hiilawe Stream drains the relatively dry southeast side of Kohala Volcano, where average annual rainfall is about half that of the wet Kohala summit (Fig. 3). It is also important that the headwall of Hiilawe Valley is presently located at the contact between Pololū and Mauna Kea basalts (Fig. 3). Headwall retreat might have stalled at this geologic contact because Mauna Kea basalt is younger and possibly less weathered and more resistant to erosion than Kohala basalt.

In contrast to Hiilawe Valley (valley 1), amphitheater-headed valleys 4–7 (Fig. 1) have headwalls located many kilometers from the present-day sea cliffs, but the drainage areas that feed their waterfalls are less than 5 km^2—values typical of the hanging and intermediate valleys. We speculate that these valleys are inactive and that headwall migration occurred in the past when drainage areas were larger. The drainage areas to these valley headwalls have declined in time because (1) the headwalls have cut into their own contributing areas as they have migrated upstream, and (2) dominant streams (particularly valleys 2 and 3) have pirated the drainage that once flowed to valleys 4–7. As an example of the latter point, the headwall of Waimanu Valley (valley 6) is ~4 km inland from the sea cliffs, although its present-day drainage area is only 0.58 km^2. It does not appear to have an actively eroding headwall because it is mantled with talus (Kochel and Piper, 1986) and plunge pools are not well developed. Examination of the topography clearly shows that Waipi‘o Valley (valley 2) has cut across the headwall of Wiamanu Valley and captured its drainage (Fig. 1). This suggests that Waimanu Valley formed before it was truncated by Waipi‘o Valley. After truncation, the contributing drainage to Waimanu Valley has been insufficient to transport the coarse debris at its headwall and cause further headwall propagation (despite active seepage flow of 0.22–0.52 m^3/s; Table 1). While the piracy of Waimanu (valley 6) by Waipi‘o (valley 2) is visually the clearest example in Figure 1, it is possible that all of the eastern amphitheater-valley heads (e.g., valleys 5–7) have lost some drainage to Waipi‘o (valley 2), and that Pololū Valley (valley 4) and West Honokāne Valley have lost drainage to the eastern head of Honokāne (valley 3). This can be seen by analyzing current drainage paths (perpendicular to contours) on Figure 1.

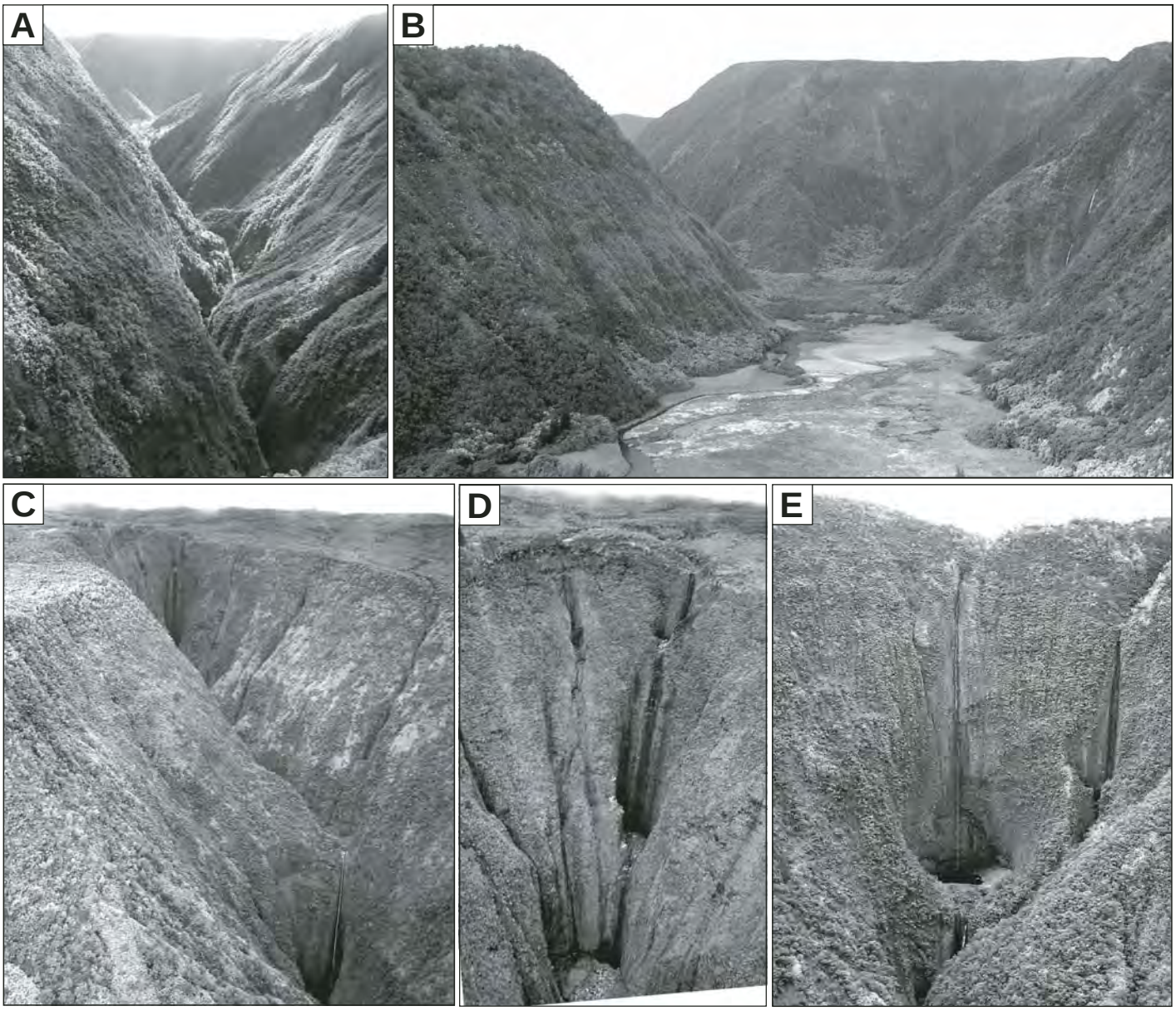

Figure 8. Photographs of Kohala amphitheater-headed canyons. (A) Upslope portion of Waipi‘o Valley showing V-shaped cross section (near c3 in Figs. 1 and 7). For scale, the valley relief shown in the image is ~700 m. (B) Mouth of Waipi‘o Valley showing U-shaped cross section (near c1 in Figs. 1 and 7). The valley relief shown is ~350 m. (C) Headwall of Waipi‘o Valley (valley 2). The total headwall relief shown is ~ 500 m. (D) Close-up of headwall of Waipi‘o Valley (valley 2) showing multiple plunge pools vertically drilling into the rock. The headwall relief in the image is ~ 350 m. (E) Upper ~300 m of the East Honokāne headwall (valley 3) showing plunge pool drilling as well as undercutting.

In order to quantitatively test whether there is a correlation between drainage area and knickpoint propagation rate, it would be ideal to have a record of drainage area to the knickpoints before significant headwall retreat and stream piracy. Unfortunately, this is not possible since headwall propagation has changed drainage patterns through time. This notwithstanding, it is encouraging for the plunge-pool erosion hypothesis that the two valleys (valleys 2 and 3) that appear to have the most actively eroding plunge pools also have two of the largest drainage areas and headwall propagation distances, and the drainage areas to these valley heads are about twice as large as those to the hanging and intermediate valleys. If valleys 2 and 3 are truly the only active amphitheater-headed valleys, then a threshold drainage area of ~5–8 km^2 might be necessary for knickpoint propagation on Kohala.

The dominance of valleys 2 and 3 over the hanging and intermediate valleys (and perhaps over the other amphitheater-headed valleys) is at least partially due to the faults near the Kohala summit (Fig. 1). While we argued previously that they do not represent the headscarp of the Pololū Slump, these faults clearly have influenced drainage to the Kohala valleys. The faults cut off the headwaters of the hanging valleys and funnel this drainage laterally to the

amphitheater-headed valleys. The fact that the amphitheater-headed valleys are developed only on the edge of this fault scarp, combined with the observation that the hanging valleys are bordered upslope by the fault scarp, suggests that this drainage divide encouraged the amphitheater-headed valleys to grow at the expense of the hanging valleys.

The Kohala amphitheater-headed valleys cut through the Pololū volcanic series and therefore must be younger than ca. 250 ka. Some of the valleys formed before the cessation of Hawi volcanic series (ca. 130 ka) and Mauna Kea volcanic series (ca. 65 ka) because Hawi flows poured into the heads of Pololū Valley (and were later incised; Macdonald et al., 1983) and East Honokāne Valley (valley 3) (Wolfe and Morris, 1996), and Mauna Kea volcanic rocks filled the head of Hiilawe valley (valley 1) (Fig. 3). If the estimated fill of 600–700 m in Waipi‘o Valley is correct, then such incision implies that the valley headwall must have propagated upstream on the order of several kilometers or more when sea level was lower than present by 600–700 m (Fig. 1). This suggests that headward erosion of Waipi‘o Valley began shortly after the cessation of the Pololū volcanic series (ca. 250 ka) when Kohala Volcano was an additional 650 m above sea level (i.e., 250 ka × 2.6 mm/yr = 650 m). This would place the valley initiation time appropriately close to the age of the Pololū Slump.

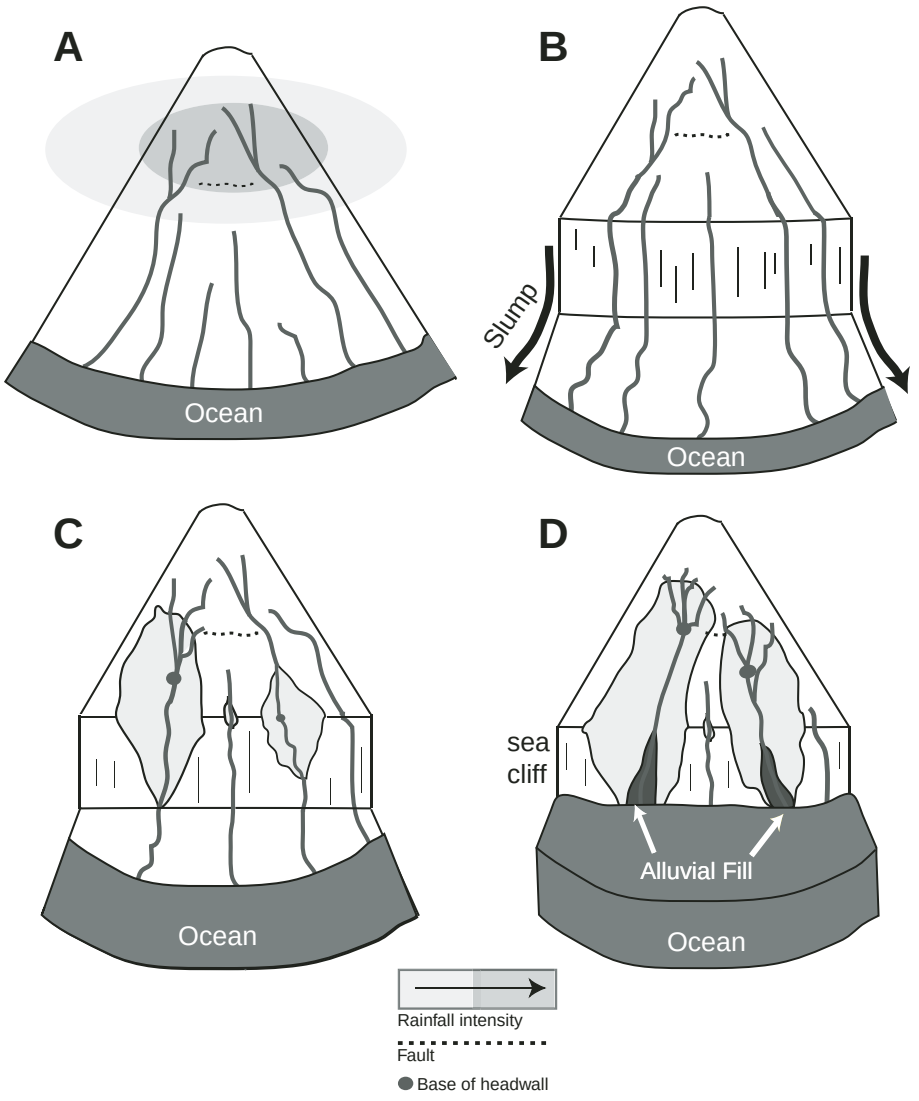

Figure 9. Conceptual model for the formation of the Kohala amphitheater-headed canyons. (A) Variable topography, lithology, orographic precipitation, fault-induced drainage divides, and a radial drainage pattern lead to dominant streams. (B) The Pololū Slump imposes giant knickpoints onto the streams. (C) Knickpoints propagate in dominant streams and through plunge-pool erosion and mass wasting capture the headwaters of neighboring valleys. Smaller valleys remain hanging at the slump headscarp. (D) Rising sea level floods the lower portions of the valley floors causing sedimentation and U-shaped valley cross sections.

CONCEPTUAL MODEL

The large Kohala amphitheater-headed valleys are directly upslope from and are laterally bounded at their outlets by the Pololū Slump and the Kohala sea cliffs (Fig. 2). Based on this spatial correlation and the coincident timing discussed previously, we propose that the Pololū Slump (rather than seepage erosion) created large knickpoints in pre-existing stream profiles. Further, we suggest, based on our field observations of plunge-pool erosion, that waterfalls (rather than seepage) caused the upstream migration of these knickpoints to form the amphitheater-headed valleys.

Before the Pololū Slump, several factors might have led to the development of dominant streams (Fig. 9A). In any drainage network, nonuniform topography, lithology, and precipitation cause some streams to capture more drainage area than others. Fault scarps near the summit of Kohala force high-elevation drainage to flow laterally, diverting runoff toward valleys at the northwest and southeast edges of the slump zone. Orographic variation in rainfall across the volcano is presently significant (Fig. 3) and was likely even greater when the volcano was an additional 1000 m above sea level. Due to the fault scarp and the radial drainage pattern, only a few streams receive high-elevation runoff, and due to orographic effects, precipitation is greater at high elevations, leading to the dominance of streams with their source regions near the summit.

Circa 250 ka, the Pololū Slump imposed giant knickpoints on the streams (Fig. 9B). We propose that waterfalls in dominant streams had sufficient sediment and water discharge to cause the knickpoints to propagate upstream through waterfall erosion (Fig. 9C). As discussed already, observations of the valley headwalls suggest that vertical drilling into the rock by the falling water and sediment is a dominant headwall erosion process. Mass failures likely also contribute to headwall propagation and probably result from plunge-pool undercutting and failure of the narrow ridges in between plunge pools (Stearns, 1985). Despite failures, horizontal bedding and vertical fracturing of the basalt promote a relatively stable headwall and thus preserve the amphitheater shape of the propagating valley heads (Stearns, 1985; Dunne, 1990). Storm-induced runoff events

are necessary to evacuate collapsed material and allow headwall propagation to continue.

Bedrock can be eroded within a plunge pool through plucking of fractured blocks due to cavitation or differential fluid pressure and abrasion due to impacting sediment (Whipple et al., 2000). Plucking might be particularly important if the bedrock is well fractured (e.g., Bollaert and Schleiss, 2003). If the rock is massive, then abrasion is expected to dominate erosion (Whipple et al., 2000). Sediment might abrade the bedrock within a plunge pool due to the initial impact and later impacts as the turbid water is churned within the pool.

As a waterfall drills a plunge pool, erosion must eventually cease when the plunge pool is approximately level with the valley floor. At this point the valley floor slope is too gentle to transport sediment away from the headwall and the plunge pool becomes armored with sediment. In order for retreat of the headwall to continue via vertical plunge-pool incision, a new plunge pool must be initiated. Thus, the creation of steps that lead to plunge pools might be a rate-limiting process for headwall retreat. We speculate that steps on the face of the headwalls form as weaker beds (e.g., interbedded ash layers) are weathered and attacked by surface runoff. Many small subhorizontal steps of protruding basalt beds can be seen at a variety of elevations at valley headwalls (Fig. 8). Prominent steps might eventually form plunge pools as they are bombarded by falling water and sediment. The abundance of protruding beds and plunge pools at different elevations at a single valley headwall (e.g., Fig. 8D) suggests that plunge pools form frequently.

As a headwall propagates upstream, the radial drainage pattern induced by the dome shape of the volcano allows the capture of the headwaters of other streams. Multiple waterfalls and mass wasting of narrow ridges in between plunge pools propagate a headwall that is much wider than any individual stream (e.g., Fig. 8D). Mass wasting along valley sidewalls also captures neighboring drainage (e.g., Hovius et al., 1998). Valley-wall slopes are reduced to a near-constant 50°, where presumably vegetation growth aids stability (Scott and Street, 1976). Crosscutting of smaller valleys by amphitheater-headed valleys has been used as evidence for seepage erosion in Hawai'i (Kochel and Piper, 1986; Kochel and Baker, 1990) and elsewhere (e.g., Hoke et al., 2004). This need not be the case because such crosscutting relationships are expected to result from headwall propagation due to waterfall erosion and mass wasting (Macdonald et al., 1983). As discussed above, the Kohala drainage is strongly influenced by faults, which appear to control the orientation of the heads of Waipi'o and Honokāne Valleys. It is possible that some of the crosscutting relationships (e.g., Waipi'o crossing Waimanu Valley) were caused by rerouting of drainage due to these faults.

Shortly after failure of the Pololū Slump, the headwalls might have been more pointed or V-shaped in planform than currently because the streams upslope of the headwalls would have had larger drainage areas and higher erosion rates (Fig. 9C). For example, the intermediate Honopue Valley (valley 8) has a pointed headwall in planform because of substantial incision upslope of the knickpoint (Fig. 1). As the headwalls propagate upstream, they progressively cut into their own drainage areas, resulting in reduced water and sediment discharge. Near the volcano summit, streams feeding the amphitheater-headed valleys are not significantly incised, and therefore the amphitheater headwalls tend to be more U-shaped in planform. For headwalls near the summit, mass failures might become more important than previously for generating sediment that acts as abrasion tools within plunge pools. Eventually, as drainage area diminishes, headwall propagation by waterfall erosion will cease. Weathering and mass wasting then become dominant processes for headwall erosion (e.g., Young, 1985; Weissel and Seidl, 1997), likely resulting in talus deposition at the base of the headwall. If hillslope processes cause the headwall slope to relax at the same rate as the valley walls, then the amphitheater shape will maintain even if the headwall is no longer actively retreating (e.g., Howard, 1995).

Long profiles of the Kohala valley floors are generally concave-up downstream of valley headwalls (Fig. 6), indicating an increasing channel slope with decreasing drainage area. The slope of the streambed is probably set by the ability of the stream to transport coarse sediment (Sklar and Dietrich, 2006). If sediment cannot be removed from the base of the headwall, deposition will occur, and the streambed slope will increase until sediment transport can occur. Transport of sediment away from the headwall, therefore, is a fundamental control on the height of the headwall as it propagates upstream. As relative sea-level rises, the valley floor becomes graded to sea level, transitioning to an alluvial-mantled reach. Subsidence eventually submerges the lower reaches of the valleys, which forces deposition and U-shaped valley cross sections (Fig. 9D).

Most of the Kohala valleys are widest near their mouths and narrow slightly headward. This, however, is not true of Honokāne Valley, which widens headward (Fig. 1). Headward widening is significant because it is thought to be a characteristic of seepage erosion (e.g., Higgins, 1984). Since the Kohala valleys are V-shaped in cross section and have near-uniform sidewall slopes, geometry requires that valleys with more relief are also wider. This appears to be the case for Honokāne Valley. Headward widening of Honokāne correlates with a headward increase in relief because the volcano surface is steeper than the valley floor (Fig. 6). As discussed already, the ability of a stream to transport sediment governs the valley-floor slope, which in turn sets valley relief. Thus, headward widening of Honokāne valley might simply be a result of a headward increase in valley relief and does not necessarily indicate seepage erosion.

Smaller streams have not produced migrating knickpoints because they have smaller drainage areas (<5 km^2), and therefore insufficient water and sediment discharge to cause knickpoint retreat. The threshold might exist because the waterfalls are not able to initiate the step-forming process, pluck blocks from the plunge pools, transport deposited sediment out of plunge pools, or transport sediment to the plunge pools. These mechanisms are discussed in more detail in the section "Thresholds for Headwall Propagation."

If the knickpoints were initiated by the Pololū Slump ca. 250 ka at the approximate location of the present-day sea cliffs, then an average knickpoint migration rate can be calculated. Here, we make this calculation for valleys 2 and 3 since they arguably have the most active valley heads. Dividing migration distance (Table 1) by 250 ka yields average headwall migration rates of 60 and 47 mm/yr for valleys 2 and 3, respectively. These rates are large but not unreasonable. For example, average waterfall retreat rates in excess of 1 m/yr have been documented for Niagara Falls, United States (Gilbert, 1907; Philbrick, 1974), Ryumon Falls, Japan (Yoshida and Ikeda, 1999), and various waterfalls in Scotland (Bishop et al., 2005).

SCALING OF PLUNGE-POOL EROSION

Waterfall propagation is typically thought to occur in layered material through undercutting of a weak layer and the subsequent collapse of an overlying strong layer (e.g., Gilbert, 1907; Holland and Pickup, 1976). Many bedrock waterfalls, however, are not undercut, which sheds doubt on the universality of this model (Young, 1985). In fact, the validity the waterfall-undercut model has even been questioned in its most prominent field example, Niagara Falls, United States (Philbrick, 1974). It has been proposed, instead, that waterfalls retreat by fatigue and mass failure, and water only sweeps material away that would otherwise buttress the headwall (e.g., Young, 1985; Seidl et al., 1996; Weissel and Seidl, 1997). Nonetheless, most quantitative models treat waterfall propagation as a fluvial incision process using drainage area

(Hayakawa and Matsukura, 2003; Crosby and Whipple, 2006) or stream power (Howard et al., 1994; Rosenbloom and Anderson, 1994; Seidl et al., 1994; Whipple and Tucker, 1999; Bishop et al., 2005) as the driver for knickpoint propagation. While these models might simulate an upstream-propagating wave in the landscape, they do not explicitly include the processes that we observe at the Kohala waterfalls, mainly, vertical plunge-pool erosion and mass wasting.

Here, we propose a simple quantitative expression for headwall propagation. Our current level of knowledge does not permit a complete model of headwall retreat involving mass failures due to plunge-pool undercutting, drilling, and weathering. We instead focus solely on developing scaling relationships for vertical plunge-pool incision. While this paints an incomplete picture, it is a useful exercise because vertical plunge-pool erosion might be the driver for headwall propagation on Hawai'i and, to our knowledge, it has not been described in detail before. For simplicity, we only consider abrasion due to the initial impact of particles falling over a waterfall. We neglect possible contributions of plunge-pool wear due to plucking of fractured bedrock or abrasion by secondary impacts of particles as they are circulated within a turbulent pool.

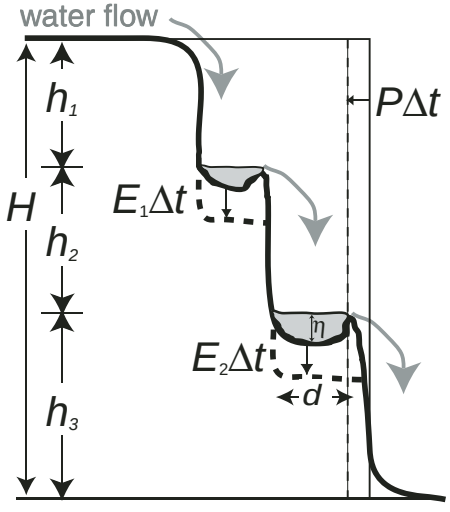

Figure 10. Schematic diagram of vertical plunge-pool erosion resulting in net upslope headwall retreat as given by Equation 4. There are two plunge pools (m = 2) of depth η for the particular case shown. Vertical erosion in each plunge pool acts over an area, per unit width, d, assuming the plunge pools are of roughly the same diameter. After a time Δt (shown by dashed lines), a net volume of eroded material per unit width is given by $(E_1 + E_2)d\Delta t$, or equivalently $mEd\Delta t$, where E is the average plunge-pool erosion rate. As shown by the thin lines, this eroded volume is equivalent to a headwall propagation rate P acting over the total area of the propagating headwall (per unit width) H in time Δt. Note that the sum of the heights of the waterfalls is equal to the total height of the headwall, or equivalently the product of the average waterfall height h and the total number of waterfalls (i.e., $h_1 + h_2 + h_3 = H = [m + 1]h$).

Sklar and Dietrich (2004) developed a model for the abrasion of a bedrock river bottom by impacting particles, which we adopt here for the case of a plunge pool. The rate of vertical bedrock erosion E (LT^{-1}) can be written as

$$E = \frac{q_s}{V\delta}\frac{\varepsilon}{\kappa}\left[1-\frac{q_s}{q_t}\right]. \quad (1)$$

The first ratio on the right-hand side of Equation 1 represents the rate of particle impacts per unit bedrock area, where q_s is the volumetric flux of sediment that impacts the bed per unit width, V is the volume of an impacting particle, and δ is the bedrock area per unit width over which impacts occur (Table A1). The second ratio on the right-hand side of Equation 1 represents the volume of bedrock eroded per particle impact, where ε is the kinetic energy of a particle impact, and κ is the energy required to detach a unit volume of bedrock (energy/volume). κ is a measure of the capacity of the bedrock to store energy elastically and depends on the tensile yield strength of the rock and Young's modulus of elasticity (Sklar and Dietrich, 2004). Equation 1 assumes that there is not a threshold kinetic energy necessary to cause abrasion, which has been verified experimentally (Sklar and Dietrich, 2001). The last ratio on the right-hand side of Equation 1 accounts for alluvial coverage that protects the bedrock from erosion, where q_t is the volumetric sediment-transport capacity of the flow per unit width. For the case of a plunge pool, q_t is the maximum sediment flux per unit width that the waterfall is able to transport out of the pool. Bedrock erosion is zero when the sediment supply exceeds the flow's capacity to transport sediment (i.e., deposition occurs).

The kinetic energy of a falling particle is given by

$$\varepsilon = \frac{1}{2}\rho_s V w_f^2, \quad (2)$$

where w_f is the vertical velocity of a particle when it collides with the bedrock, and ρ_s is the particle density. If we define d as the surface area of the floor of the plunge pool per unit width, then Equations 1 and 2 can be written for the case of a plunge pool as

$$E = \frac{q_s}{2d}\frac{\rho_s w_f^2}{\kappa}\left[1-\frac{q_s}{q_t}\right]. \quad (3)$$

The volumetric flux of bedrock lost (per unit width) from a headwall due to plunge-pool erosion can be written mEd, where m is the number of successive plunge pools stacked vertically above one another for an average contributing stream (Fig. 10). This implicitly assumes that E is an average or characteristic vertical erosion rate for m successive plunge pools. m does not include the plunge pool at the base of the headwall, since presumably this pool is not vertically incising and therefore does not contribute to headwall retreat. For the purpose of formulating an average headwall propagation rate, this vertical flux of material can be written as a horizontal flux averaged over the entire surface area of the headwall (per unit width) by continuity as

$$mEd = HP, \quad (4)$$

where H is the height of the propagating headwall, and P is the inferred average headwall retreat rate due solely to vertical plunge-pool erosion (Fig. 10).

Equations 3 and 4 now can be combined for the rate of headwall propagation due to vertical plunge-pool erosion,

$$P = \frac{mq_s}{2H}\frac{\rho_s w_f^2}{\kappa}\left[1-\frac{q_s}{q_t}\right]. \quad (5)$$

In order to better illustrate the dependencies of headwall propagation, it is useful to use the fact that the product of the total number of waterfalls in series (i.e., m + 1, which is one more than the total number of plunge pools contributing to erosion m) and their average fall distance, h, is equal to the total height of the headwall (i.e., $H = [m + 1]h$) (Fig. 10). In addition, if it is assumed that the average plunge-pool depth, η, is much smaller than the waterfall height (i.e., $h >> \eta$), then $h \approx h + \eta$ and Equation 5 can be written as

$$P = \frac{\rho_s g q_s}{\kappa}\left[1-\frac{q_s}{q_t}\right]\left[\frac{m}{m+1}\right]\left[\frac{w_f^2}{2g(h+\eta)}\right]. \quad (6)$$

Equation 6 is preferred over Equation 5 because it illustrates that, in addition to sediment supply q_s, sediment density ρ_s, and rock erodibility κ, headwall propagation is a function of the three nondimensional ratios, with

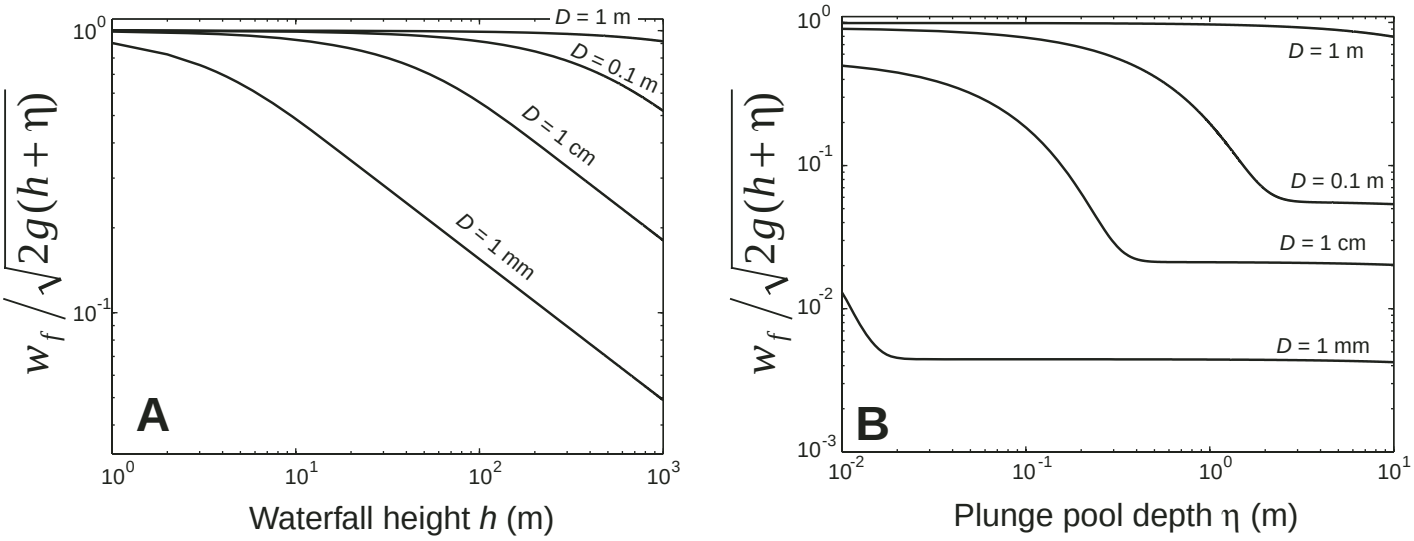

Figure 11. Plot of particle impact velocity as given by Equation A9 (w_f) normalized by the impact velocity assuming no drag (Equation 8) for different particle diameters *D*. Equation A9 is evaluated for the conditions of (A) different waterfall heights *h* and zero plunge-pool depth η and (B) a constant waterfall height of 100 m and variable plunge-pool depths. The calculation assumes that the density of sediment = 2800 kg/m^3, the density of water = 1000 kg/m^3, and the density of air = 1.275 kg/m^3. The particles are assumed spherical, so that $V/A = 2D/3$. The drag coefficient C_d was calculated for natural spherical particles at terminal settling velocity using the formula of Dietrich (1982). See Appendix 1 and Table A1 for more detail.

values between zero and unity, shown in brackets. These are (1) the sediment supply versus transport capacity of the plunge pools, (2) the existence and relative number of plunge pools, and (3) the kinetic versus potential energy of sediment impacts. Note that headwall propagation given by Equations 5 and 6 is predicted to be independent of the surface area of the plunge pools *d*.

Equations 3 and 6 predict that the rates of vertical plunge-pool erosion and headwall propagation depend (nonlinearly) on the flux of sediment that passes over the waterfall. Sediment flux is positively correlated with the rate of conversion of rock to sediment from the valley walls and channel bed upslope of the waterfall, and the drainage area of the basin that contributes to the waterfall. Sediment flux also depends inversely on the recurrence interval of sediment-transporting events in the stream upslope of the waterfall (e.g., Sklar and Dietrich, 2006). Given that the production of sediment and the recurrence interval of storm events are probably similar for different Kohala amphitheater-headed valleys because of similar bedrock lithology and climate (except for valley 1), Equations 3 and 6 are in qualitative agreement with our Kohala observations that valley headwalls with relatively large contributing drainage areas appear to have better-developed plunge pools and faster headwall retreat rates.

While sediment can abrade rock, it also can protect bedrock from erosion if deposition occurs (e.g., Sklar and Dietrich, 2001). As shown in the first bracketed ratio on the right-hand side of Equation 6, the headwall propagation rate is predicted to trend to zero as sediment supply approaches the sediment transport capacity of a waterfall plunge pool. To our knowledge, the sediment transport capacity of a plunge pool has yet to be assessed. It is likely to be different than the simpler and better studied unidirectional case due to complex three-dimensional flow of the impinging jet. For example, as a plunge pool grows in depth, the ponded water slows the impact velocity of the falling particles and dissipates energy of the plunging water. If deposition occurs, the downstream lip of the plunge pool might need to be incised so that sediment can be transported out of the pool and erosion can continue.

The formation of plunge pools (i.e., the functional form of *m*) is critical to our hypothesis of erosion by vertical plunge-pool drilling. The second bracketed ratio on the right-hand side of Equation 6 shows that headwall propagation is only weakly dependent on the number of plunge pools *m* for large *m*. *m* must be greater than zero, however, for headwall propagation by waterfall drilling to occur. As discussed in the Conceptual Model section, *m* is a function of step formation, which in turn probably depends on heterogeneity of rock strength at the headwall, the magnitude of differential weathering, and the discharge of water and sediment pouring down the face of the headwall. The mechanics of step formation, however, remain unclear. In order for Equation 6 to be a valid representation of headwall retreat, we must assume that the formation of steps is not a rate-limiting process, so that $m > 0$ at all times. This appears to be a reasonable assumption in Hawai‘i since most headwalls have several active plunge pools and many protruding beds that could become plunge pools (Fig. 8D). Typical values of *m* for the Kohala valleys are between 1 and 10. Implicit in Equation 6 is the assumption that steps are generated at the top of the headwall. This also seems reasonable, as there are many steps that occur near the top of the headwalls (e.g., Fig. 8D), and there does not appear to be a critical fall distance necessary to generate steps. In reality, however, steps can develop below the top of the headwall if the overlying rock is removed by weathering and mass wasting (processes neglected in this scaling analysis).

The third bracketed ratio on the right-hand side of Equation 6 represents the ratio of kinetic versus potential energy of a particle impact, which is a function of the amount of energy lost to drag. The impact velocity increases as the height of the waterfall increases until drag on the particle causes it to approach terminal velocity. In Appendix 1, we derive an expression (Equation A9) for the fall velocity of a particle considering the effects of air drag and drag induced on the particle within the ponded water of a plunge pool. The solution to Equation A9, shown in Figure 11, indicates that drag is important for small

particle diameters, D, large waterfall heights, h, and large plunge pool depths, η (Fig. 11). For waterfall heights typical of the Kohala valleys ($h \sim 100$ m), air drag has only a minor effect on particle-fall velocity for $D \geq 10$ cm and reduces the fall velocity by approximately a factor of two for $D \approx 1$ cm (Fig. 11A). Drag within the plunge pool, however, is much more significant than air drag and must be taken into account for $D < \sim 1$ m when $\eta > \sim 1$ m (Fig. 11B). For $D <$ 10 cm and $\eta > \sim 1$ m, particles approach terminal velocity within the plunge pool, and Equation A9 can be reduced to

$$w_f = \sqrt{\frac{4(\rho_s - \rho_w)}{3\rho_w}\frac{gD}{C_d}}, \quad (7)$$

where g is the acceleration due to gravity, and ρ_w is the density of water. C_d is a drag coefficient, and it depends on the particle Reynolds number (e.g., Dietrich, 1982). Insertion of Equation 7 into Equation 6 reveals that headwall propagation is linearly dependent on the particle size and inversely dependent on the waterfall height for drag-dominated particles.

On the other hand, both air drag and plunge-pool drag are predicted to be negligible for large particle sizes ($D > 10$ cm) and small plunge-pool depths ($\eta < 10$ cm) (Fig. 11). Drag might be further reduced in air due to downdrafts caused by the falls (Young, 1985) and in plunge pools due to the vertical velocity of the impinging waterfall and aeration of the pool. If drag can be neglected, then the impact velocity can be approximated by assuming full conversion of potential energy to kinetic energy,

$$w_f = \sqrt{2g(h+\eta)}, \quad (8)$$

and therefore the third bracketed ratio in Equation 6 is unity. Interestingly, for this case, headwall propagation is predicted to be independent of particle size, waterfall height, and the total headwall height. This is because the energy of the sediment impacts depends linearly on waterfall height and so does the volume of rock that must be eroded for the headwall to propagate a unit distance. Note, however, that a single larger particle is still expected to erode more bedrock than a single smaller particle because the larger particle constitutes a greater sediment flux.

PREDICTION OF HEADWALL PROPAGATION RATE

It is not yet possible to use Equation 6 in a landscape evolution model because there are several terms with unknown functional dependencies, most notably m and q_t. We can, however, estimate a maximum headwall propagation rate by assuming that (1) plunge pools are abundant, and their formation is not rate limiting (i.e., $m \gg 0$), (2) particle-fall velocities are unaffected by drag (i.e., Equation 8), and (3) sediment supply is much less than the sediment-transport capacity of the plunge pools (i.e., no coverage of bedrock, $q_s \ll q_t$). With these assumptions, the three bracketed ratios on the right-hand side of Equation 6 are unity, and Equation 6 reduces to a maximum propagation rate

$$P_{max} = \rho_s g q_s / \kappa. \quad (9)$$

The maximum headwall propagation rate predicted by Equation 9 can now be compared with the average propagation rates found for Waipi‘o and Honokāne Valleys (i.e., valleys 2 and 3) of 60 mm/yr and 47 mm/yr to see if the model yields a reasonable prediction.

Unfortunately, there is much uncertainty in determinations of both the average sediment flux passing over the waterfall, q_s, and the erosion parameter, κ. If the valley dimensions upstream of the headwalls were known, then the average sediment flux over a waterfall could be estimated by neglecting dissolution and erosion of interfluves and assuming that all valley erosion upstream of an amphitheater head produces sediment that is transported over the waterfall, i.e.,

$$q_s w = A_v L_v / \Delta t, \quad (10)$$

where A_v is the average cross-sectional area of a valley upstream of a headwall, L_v is the cumulative valley length upstream of the headwall (averaged in time), Δt is the change in time over which valley incision occurred, and w is the width of the channel at the waterfall. It is not possible to quantify the valley dimensions upstream of the Kohala amphitheater headwalls because the valleys have been erased as the headwalls have propagated upstream, effectively reducing L_v in time. For valleys 2 and 3, we estimate L_v, currently to be ~4 km and at the time of the Pololū Slump to have been on the order of 20 km (Fig. 6). We use these end-member values to calculate an average or effective L_v of ~8 km (i.e., [20 km – 4 km]/2). To make an estimate of sediment flux, we assume a valley cross-sectional area (averaged in space and time) to be triangular with a width of ~300 m and a depth of ~100 m, yielding $A_v = 15{,}000$ m^2. These dimensions seem reasonable based on a rough survey of some of the larger hanging valleys. We set Δt to the approximate age of the Pololū Slump (i.e., $\Delta t = 250$ ka), estimate the stream channel width $w = 5$ m, and calculate q_s = 96 m^2/yr from Equation 10. While these estimates are rough, they are unlikely to be off by more than a factor of two or three. There is significantly more uncertainty in the estimate of κ.

Sklar and Dietrich (2004) define $\kappa = k\sigma_T^2/2Y$, where σ_T is the rock tensile strength, Y is Young's modulus of elasticity (~10^5 MPa; Selby, 1993), and k is an empirical nondimensional constant ($k \approx 10^6$ based on laboratory experiments of Sklar and Dietrich [2001], which, to our knowledge, has not yet been tested at field scale). For most rock types, σ_T varies from ~1 to 20 MPa (Selby, 1993). At the laboratory scale, intact basalt might have a tensile strength around 10 MPa, although weathering and fracturing in the field could lower this estimate by an order of magnitude or more.

Given this uncertainty, we solve Equations 9 and 10 for a range in rock tensile strengths using the values specified above, and $\rho_s = 2800$ kg/m^3. The result of this calculation yields $P_{max} = 5.3$–530 mm/yr for $\sigma_T = 1$–10 MPa. These values bracket the inferred average propagation rates of 60 mm/yr and 47 mm/yr for valleys 2 and 3. While there is much uncertainty in this calculation, it is encouraging that the model yields feasible headwall propagation rates that compare well with observed rates, despite the fact that mass wasting, plucking, and erosion from churning of sediment within a plunge have been neglected.

THRESHOLDS FOR HEADWALL PROPAGATION

We hypothesized in the Conceptual Model section that some valleys have remained hanging at the Kohala sea cliffs because they have had insufficient water or sediment discharge to cause headwall propagation. Here, we elaborate on possible mechanisms that might explain the possible drainage area threshold for headwall propagation of 5–8 km^2. First is the formation of plunge pools. If $m = 0$, then headwall propagation will not occur. It is difficult to assess this possibility given our ignorance of the step-formation process. Nonetheless, it seems reasonable that the hanging valleys might experience insufficient discharges of water or sediment to initiate and renew plunge pools. A second possible threshold is through the sediment-capacity term q_t. If a waterfall is unable to transport the supplied sediment out of the plunge pools and away from the valley head, then deposition will occur, and erosion will cease (i.e., $q_s > q_t$ in Equation 6). Thus, it is possible that the hanging valleys have not had sufficient discharge to evacuate the sediment delivered by mass failures or from upstream.

The third possible threshold is through the sediment-flux term q_s. The sediment flux at a waterfall during a particular flow event depends

not only on the production rate of sediment (as discussed already), but also on the ability of the flow upslope of the waterfall to mobilize that sediment. Sediment mobility is typically expressed through a nondimensional Shields number (e.g., Buffington and Montgomery, 1997). For coarse grains of similar density, the median particle size that can be transported depends linearly on the flow depth and the bed slope. Given the similar slopes of the Kohala valleys upslope of the knickpoints, it is possible that the hanging valleys have remained hanging because they have had insufficient discharge or flow depth to mobilize the coarse sediment found on their beds, effectively setting $q_s = 0$ in Equation 6. Unfortunately, we do not yet have exposure ages or sediment-transport data to test whether sediment is immobile in the Kohala hanging valleys. The possibility of relatively immobile sediment in the hanging valleys, however, seems reasonable. For example, Seidl et al. (1994, 1997) showed that large boulders that line streams on Kaua‘i (of similar slope and lithology as the Kohala valleys) have been immobile for as long as 180 k.y. based on cosmogenic exposure dating.

If sediment is presently immobile in the hanging valleys, this must not have always been the case. The hanging valleys are topographic depressions and were at one time carved by flows capable of transporting sediment. How did such flows carve the valleys without causing headward retreat at the knickpoint? It is possible that fluvial erosion in the hanging valleys only occurs as boulders and bedrock in the channels weather to small transportable pieces, which do not cause appreciable plunge-pool erosion because of small impact velocities due to drag (cf. Equation 7) or viscous damping (e.g., Schmeeckle et al., 2001). Another possibility is that the hanging valleys were carved before knickpoints were imposed on the streams by the Pololū Slump. Before the slump occurred, the hanging valleys would have had greater discharges because of higher precipitation rates (because the volcano was an additional 1000 m above sea level) and larger drainage areas (because there might not have been fault-induced drainage divides near the Kohala summit).

Lastly, it is possible that knickpoint propagation has occurred for the hanging valleys, but that it has not kept pace with coastal cliff retreat from wave erosion. Wave erosion is an active process as evidenced by sea stacks and 20–50 m sea cliffs along the entire northeast shoreline of Hawai‘i. Dividing the sea-cliff relief (20–50 m) by the regional volcano slope (~0.1) indicates at least 200–500 m of horizontal sea-cliff retreat. This retreat distance is a minimum because some portion of the sea cliffs might now be submerged due to island subsidence. Valleys will therefore remain hanging at the coast if headwall retreat rates are less than ~500 m/250 k.y., or ~2 mm/yr. A similar mechanism has been proposed for the difference between hanging and amphitheater-headed valleys on the coast of New Zealand (Pillans, 1985).

OTHER HAWAIIAN VALLEYS

Large submarine landslides are found offshore of Kaua‘i, O‘ahu, Moloka‘i, Maui, and Hawai‘i. When they occur on the windward wet sides of the islands, the landslides are often associated spatially with amphitheater-headed valleys (Moore et al., 1989; Moore and Clague, 1992). Clague and Moore (2002) suggested that this might be a coincidence since both landslides and deep valleys likely require high precipitation rates. Landslides might be triggered by groundwater-induced pressurization caused by magma intrusion or phreatomagmatic eruptions (Clague and Moore, 2002), and amphitheater-headed valleys are generally found in areas where annual precipitation exceeds 2.5 m (Scott and Street, 1976). Moore et al. (1989), however, suggested that the amphitheater-headed valleys might be genetically linked to the landslides, as the landslides could have caused “oversteepening” or removed vegetation. Like our interpretation for Kohala, Seidl et al. (1994) argued that valleys on the Na Pali coast of Kaua‘i were carved by upstream-migrating landslide-induced knickpoints.

Amphitheater-headed valleys on the north coast of Moloka‘i, most notably Pelekunu and Wailau Valleys (Stearns, 1985), were interpreted by Kochel and Piper (1986) to have resulted from seepage erosion. Like Kohala, these valleys have incised through large sea cliffs, which have ~1000 m of relief in the region of the valleys and taper to less than ~100 m to the east and west (Clague and Moore, 2002). Directly off the north shore of Moloka‘i is the huge Wailau landslide (Moore et al., 1989). Similar to Kohala, the origin of the sea cliffs was originally attributed to wave back-cutting (Wentworth, 1928; Macdonald et al., 1983), but was later interpreted as the headwall of the Wailau landslide when bathymetric surveys revealed the slide (Moore et al., 1989; Satake and Smith, 2000). More recently, Clague and Moore (2002) suggested, based on comparison with a similar feature on Kilauea Volcano, that the sea cliffs are a result of normal or listric faulting independent of the landslide.

On Moloka‘i and the other Hawaiian Islands, the spatial correlation between landslides, sea cliffs, and amphitheater-headed valleys are generally not as clear as on Kohala, making interpretations more difficult. This might be because the other islands are older and have experienced a more complicated relative sea-level history (e.g., Dickinson, 2001). Erosion of some amphitheater-headed valleys has progressed to the point that they have coalesced, making it difficult to distinguish where valleys once were (e.g., on Kaua‘i; Stearns, 1985). It does seem plausible, however, that large sea cliffs were formed by giant mass failures at least on Moloka‘i and Kohala. Even if the sea cliffs on these islands were created by faulting unrelated to mass failures, the spatial correlation between amphitheater-headed valleys and large sea cliffs on the windward, wet sides of many of the Hawaiian Islands suggests a causal relationship consistent with the knickpoint-retreat model presented herein.

CONCLUSIONS

The Kohala amphitheater-headed valleys have steep, stubby headwalls that are dominated by waterfall plunge pools. These headwalls appear to be at odds with classic models of waterfall retreat because plunge pools do not coincide with significant changes in bedrock strength and headwalls are not significantly undercut. Instead, the falling water and sediment appear to be vertically drilling into the headwall in a series of steps that interrupt the cascading falls. Springs do exist in the Kohala valleys, as one would expect in any deeply incised canyon that intersects a water table. We, however, did not observe any weathered rock or overhangs associated with springs. Peak annual surface flows exceed spring discharges by nearly two orders of magnitude and are likely necessary to excavate collapsed talus. The amphitheater-headed valleys have approximately uniform valley-wall slopes, and are V-shaped in cross section in their upstream portions but are flat-floored near the valley mouths. The valleys occur directly upslope of anomalously high sea cliffs, which in turn are upslope from the Pololū Sump. Faults located near the volcano summit cause lateral (cross-slope) surface flow of high-elevation (orographically enhanced) precipitation to the amphitheater-headed valleys at the expense of smaller valleys that remain hanging at the sea cliffs.

To explain these observations, we propose that the Kohala amphitheater-headed valleys formed by upstream propagation of huge knickpoints induced by the Pololū Slump. Circa 250 ka, the Pololū Slump created an immense headscarp that is recorded presently as the > 400 m sea cliffs that laterally bound

the slump. As dominant streams cascaded over the cliffs, they developed waterfalls, which, through plunge-pool erosion and mass wasting, induced upstream propagation of knickpoints at rates up to 60 mm/yr, eventually forming deep amphitheater-headed valleys. Upstream propagation of valley headwalls resulted in crosscutting of drainage networks and stream piracy. Smaller streams did not develop into amphitheater-headed valleys because they had smaller discharges due to orographic precipitation, a radial drainage pattern, and fault-induced drainage divides near the summit of the volcano. Topographic analysis suggests a potential drainage area threshold of ~5–8 km^2 between the arguably active amphitheater-headed valleys and the inactive amphitheater-headed, intermediate, and hanging valleys. Subsidence drowned the lower portions of the amphitheater-headed valleys resulting in alluviation, flat floors, and U-shaped cross sections.

We propose a simple expression to describe headwall retreat by vertical plunge-pool erosion due to impacting sediment. This model suggests that headwall propagation and plunge-pool erosion scale with drainage area through the sediment-flux term, which is partially supported by our field observations and drainage area analysis. The rate of headwall propagation is predicted to be dependent on the kinetic versus potential energy of sediment impacts, which is a function of sediment size, plunge-pool depth, and waterfall height. Surprisingly, for large particles and small plunge-pool depths, drag can be neglected, and headwall propagation is not a function of sediment size, waterfall height, or total headwall height. Headwall propagation is only weakly dependent on the number of plunge pools and is independent of the surface area of the plunge pools. The derived expression is consistent with the notion of a threshold for headwall propagation through either the development of plunge pools, the sediment-transport competency of the streams feeding the plunge pools, or the sediment-transport capacity of plunge pools themselves. The model does not include other potential thresholds such as a waterfall's inability to pluck fractured rock from plunge pools or keep pace with coastal cliff retreat. While the model is an oversimplification, it is encouraging that it yields feasible headwall propagation rates that compare favorably with those inferred from observations.

The interpretation that the Kohala valleys formed by waterfall processes is significant because it implies that amphitheater form is not a diagnostic indicator of seepage erosion. The process of knickpoint formation and retreat following large-scale landsliding described for Kohala might also explain the origin of amphitheater-headed valleys on other Hawaiian Islands. Moreover, amphitheater-headed valleys (e.g., on oceanic islands of Vanuatu, Tahiti, and La Réunion; Karátson et al., 1999) and stepped waterfalls (e.g., Skógar River, Iceland; Cascade River, Minnesota, United States) are a relatively common occurrence on Earth, especially in basaltic landscapes. Knickpoint retreat is thought to be one of the main mechanisms for valley incision (e.g., Whipple, 2004), and the process of vertical drilling proposed herein might be relevant for landscape evolution outside of the Hawaiian Islands. Mars in particular has abundant amphitheater-headed valleys that should be reevaluated with attention to waterfall processes in addition to seepage erosion.

APPENDIX 1

The acceleration of a falling particle can be calculated from the difference between the gravitational acceleration and deceleration due to drag:

$$\frac{dw}{dt} = C_1 - C_2 w^2 , \tag{A1}$$

where w is velocity in the vertical dimension, g is the acceleration due to gravity, and C_1 and C_2 are given by

$$C_1 = \frac{\left(\rho_s - \rho_f\right)}{\rho_s} g , \tag{A2}$$

$$C_2 = \frac{1}{2} C_d \frac{\rho_f}{\rho_s} \frac{A}{V} , \tag{A3}$$

where C_d is a drag coefficient, ρ_f is the density of the fluid that the particle is falling through, ρ_s is the particle density, A is the cross-sectional area of the particle perpendicular to fall velocity, and V is the volume of the particle. We are interested in the acceleration over a certain fall distance rather than over a certain fall time. Equation A1 can be written in terms of vertical distance z (positive downward) by substituting $dt = dz/w$, which yields

$$w \frac{dw}{dz} + C_2 w^2 = C_1 . \tag{A4}$$

In order to solve Equation A4 analytically, we assume that C_2, and therefore C_d, is a not a function of z. In reality C_d should vary as particles accelerate and the particle Reynolds number increases. Using a simple numerical integration, we found that accounting for a variable drag coefficient typically has less than a 10% effect on settling velocity. We, therefore, assume that C_d is a constant for a given particle size and solve the nonlinear ordinary differential equation given by Equation A4 analytically as

$$w = \sqrt{\frac{C_1}{C_2} + C_3 \exp\left(-2C_2 z\right)} . \tag{A5}$$

C_3 is a constant of integration that must be specified using a boundary condition. Neglecting the influence of the surrounding falling water, a particle falling down a waterfall will first fall through air for a distance h and then through water within the pool for a distance η before impacting the bedrock. We first specify Equation A5 for the case of a particle falling through air. We then use this solution as the boundary condition for a particle falling through water.

For the particle falling through air, we define $C_1 = C_{1a}$ and $C_2 = C_{2a}$ for the case when $\rho_f = \rho_a$ in Equations A2 and A3, where ρ_a is the density of air. Solving Equation A5 for C_3 and assuming that the vertical velocity of the particle at the top of the waterfall ($z = 0$) is zero, yields $C_3 = -C_{1a}/C_{2a}$. Thus, the velocity of a particle when it impacts the water in a plunge pool ($z = h$), denoted by w_a, can be written following Equation A5 as

$$w_a = \sqrt{\frac{C_{1a}}{C_{2a}}\left(1 - \exp\left(-2C_{2a} h\right)\right)} . \tag{A6}$$

Now, we solve Equation A5 for the particle-bedrock impact velocity at the bottom of the plunge pool.

TABLE A1. NOTATION

A	Cross-sectional area of a sediment particle (L^2)
A_v	Average cross-sectional area of a valley upstream of a headwall (L^2)
C_d	Drag coefficient (dimensionless)
d	Surface area of a plunge pool per unit width (L)
D	Sediment diameter (L)
E	Vertical erosion rate (LT^{-1})
g	Acceleration of gravity (LT^{-2})
h	Average waterfall height for m + 1 waterfalls in series at a headwall (L)
k	Empirical rock erodibility coefficient (dimensionless)
L_v	Average length of a valley upstream of a headwall (L)
m	Number of plunge pools in series at a headwall (not including bottom of headwall)
P	Headwall propagation rate (LT^{-1})
P_{max}	Estimate of maximum headwall propagation rate (LT^{-1})
q_s	Volumetric sediment flux or supply per unit width (L^{2}T^{-1})
q_t	Volumetric sediment-transport capacity per unit width (L^{2}T^{-1})
t	Time (T)
V	Volume of a sediment particle (L^3)
w	Vertical velocity of a falling particle (LT^{-1})
w_f	Impact velocity of a particle at the bedrock interface (LT^{-1})
Y	Young's modulus of elasticity (ML^{-1}T^{-2})
z	Vertical coordinate (L)
η	Plunge pool depth (L)
κ	Rock erodibility parameter (ML^{-1}T^{-2})
ρ_s	Density of sediment (ML^{-3})
ρ_f	Density of fluid (ML^{-3})
ρ_w	Density of water (ML^{-3})
ρ_a	Density of air (ML^{-3})
σ_T	Rock tensile strength (ML^{-1}T^{-2})

For the case of a particle falling through water, we define $C_1 = C_{1w}$ and $C_2 = C_{2w}$ for the case when $\rho_f = \rho_w$ in Equations A2 and A3, where ρ_w is the density of water. At the top of the pool of water ($z = 0$), the velocity of the particle is w_a, given by Equation A6. This assumes that no energy is dissipated at the air-water interface. Given this boundary condition, C_3 is found from Equation A5 to be

$$C_3 = w_a^2 - \frac{C_{1w}}{C_{2w}}. \quad \text{(A7)}$$

Combining Equations A5 and A7 yields the impact velocity of a particle w_f after passing through a plunge pool of depth η,

$$w_f = \sqrt{\frac{C_{1w}}{C_{2w}} + \left(w_a^2 - \frac{C_{1w}}{C_{2w}}\right)\exp\left(-2C_{2w}\eta\right)}. \quad \text{(A8)}$$

The final expression for impact velocity of a particle after falling over a waterfall of height h and through a plunge pool of depth η is found by combining Equations A6 and A8,

$$w_f = \sqrt{\frac{C_{1w}}{C_{2w}} + \left(\frac{C_{1a}}{C_{2a}}\left(1-\exp\left(-2C_{2a}h\right)\right) - \frac{C_{1w}}{C_{2w}}\right)\exp\left(-2C_{2w}\eta\right)}. \quad \text{(A9)}$$

ACKNOWLEDGMENTS

This study was funded by the National Aeronautics and Space Administration (NASA) Astrobiology Institute. The manuscript was improved after constructive comments by Tom Dunne, Lewis Owen, and an anonymous reviewer.

REFERENCES CITED

Bishop, P., Hoey, T.B., Jansen, J.D., and Artza, I.L., 2005, Knickpoint recession rate and catchment area: The case of uplifted rivers in eastern Scotland: Earth Surface Processes and Landforms, v. 30, no. 6, p. 767–778, doi: 10.1002/esp.1191.

Bollaert, E., and Schleiss, A., 2003, Scour of rock due to the impact of plunging high velocity jets. Part II: Experimental results of dynamic pressures at pool bottoms and in one- and two-dimensional closed end rock joints: Journal of Hydraulic Research, v. 41, no. 5, p. 465–480.

Buffington, J.M., and Montgomery, D.R., 1997, A systematic study of eight decades of incipient motion studies, with special reference to gravel-bedded rivers: Water Resources Research, v. 33, no. 8, p. 1993–2029, doi: 10.1029/97WR03190.

Carr, M.H., and Clow, G.D., 1981, Martian channels and valleys—Their characteristics, distribution, and age: Icarus, v. 48, no. 1, p. 91–117, doi: 10.1016/0019-1035(81)90156-1.

Clague, D.A., and Moore, J.G., 2002, The proximal part of the giant submarine Wailau landslide, Molokai, Hawai'i: Journal of Volcanology and Geothermal Research, v. 113, no. 1–2, p. 259–287, doi: 10.1016/S0377-0273(01)00261-X.

Clague, D.A., Reynolds, J.R., Maher, N., Hatcher, G., Danforth, W., and Gardner, J.V., 1998, High-resolution Simrad EM300 multibeam surveys near the Hawaiian Islands: Canyons, reefs, and landslides: Eos (Transactions, American Geophysical Union), v. 79, p. F826.

Cotton, C.A., 1943, Oahu valley sculpture: A composite review: Geological Magazine, v. 80, p. 237–243.

Craddock, R.A., and Howard, A.D., 2002, The case for rainfall on a warm, wet early Mars: Journal of Geophysical Research–Planets, v. 107, no. E11, doi: 10.1029/2001/JE001505.

Crosby, B.T., and Whipple, K.X., 2006, Knickpoint initiation and distribution within fluvial networks in the Waipaoa River, North Island, New Zealand: Geomorphology, v. 82, p. 16–38.

Dalrymple, G.B., 1971, Potassium-argon ages from Pololū volcanic series, Kohala Volcano, Hawai'i: Geological Society of America Bulletin, v. 82, no. 7, p. 1997–2000, doi: 10.1130/0016-7606(1971)82[1997:PAFTPV]2.0.CO;2.

Davis, W.M., 1928, The Coral Reef Problem: American Geographical Society Special Publication 9, 596 p.

Dickinson, W.R., 2001, Paleoshoreline record of relative Holocene sea levels on Pacific islands: Earth-Science Reviews, v. 55, p. 191–234, doi: 10.1016/S0012-8252(01)00063-0.

Dietrich, W.E., 1982, Settling velocity of natural particles: Water Resources Research, v. 18, no. 6, p. 1615–1626.

Dietrich, W.E., and Dunne, T., 1993, The channel head, *in* Beven, K., and Kirkby, M.J., eds., Channel Network Hydrology: New York, John Wiley & Sons, p. 175–219.

Dunne, T., 1990, Hydrology, mechanics, and geomorphic implications of erosion by subsurface flow, *in* Higgins, C.G., and Coates, D.R., eds., Groundwater Geomorphology: The Role of subsurface Water in Earth-Surface Processes and Landforms: Boulder, Geological Society of America Special Paper 252, p. 1–28.

Gilbert, G.K., 1907, The rate of recession of Niagara Falls: U.S. Geological Survey Bulletin, v. 306, p. 1–31.

Grant, J.A., 2000, Valley formation in Margaritifer Sinus, Mars, by precipitation-recharged ground-water sapping: Geology, v. 28, no. 3, p. 223–226, doi: 10.1130/0091-7613(2000)28<223:VFIMSM>2.0.CO;2.

Gulick, V.C., 2001, Origin of the valley networks on Mars: A hydrological perspective: Geomorphology, v. 37, no. 3–4, p. 241–268, doi: 10.1016/S0169-555X(00)00086-6.

Hayakawa, Y., and Matsukura, Y., 2003, Recession rates of waterfalls in Boso Peninsula, Japan, and a predictive equation: Earth Surface Processes and Landforms, v. 28, no. 6, p. 675–684, doi: 10.1002/esp.519.

Higgins, C.G., 1984, Piping and sapping; development of landforms by groundwater flow, *in* LaFleur, R.G., ed., Groundwater as a Geomorphic Agent: Boston, Allen and Unwin, p. 18–58.

Hinds, N.E.A., 1925, Amphitheatre valley heads: The Journal of Geology, v. 33, p. 816–818.

Hoke, G.D., Isacks, B.L., Jordan, T.E., and Yu, J.S., 2004, Groundwater-sapping origin for the giant quebradas of northern Chile: Geology, v. 32, no. 7, p. 605–608, doi: 10.1130/G20601.1.

Holland, W.N., and Pickup, G., 1976, Flume study of knickpoint development in stratified sediment: Geological Society of America Bulletin, v. 87, no. 1, p. 76–82, doi: 10.1130/0016-7606(1976)87<76:FSOKDI>2.0.CO;2.

Hovius, N., Stark, C.P., Tutton, M.A., and Abbott, L.D., 1998, Landslide-driven drainage network evolution in a pre–steady-state mountain belt: Finisterre Mountains, Papua New Guinea: Geology, v. 26, no. 12, p. 1071–1074, doi: 10.1130/0091-7613(1998)026<1071:LDDNEI>2.3.CO;2.

Howard, A.D., 1995, Simulation modeling and statistical classification of escarpment planforms: Geomorphology, v. 12, p. 187–214, doi: 10.1016/0169-555X(95)00004-O.

Howard, A.D., and McLane, C.F., 1988, Erosion of cohesionless sediment by groundwater seepage: Water Resources Research, v. 24, no. 10, p. 1659–1674.

Howard, A.D., and Kochel, R.C., 1988, Introduction to cuesta landforms and sapping processes on the Colorado Plateau, *in* Howard, A.D., Kochel, R.C., and Holt, H., eds., Sapping Features of the Colorado Plateau: A Comparative Planetary Geology Field Guide: National Aeronautics and Space Administration (NASA) Special Publication 491, p. 6–56.

Howard, A.D., Dietrich, W.E., and Seidl, M.A., 1994, Modeling fluvial erosion on regional and continental scales: Journal of Geophysical Research–Solid Earth, v. 99, p. 13,971–13,986, doi: 10.1029/94JB00744.

Jones, A.T., 1995, Geochronology of drowned Hawaiian coral reefs: Sedimentary Geology, v. 99, no. 3–4, p. 233–242, doi: 10.1016/0037-0738(95)00046-B.

Karátson, D., Thouret, J.C., Moriya, I., and Lomoschitz, A., 1999, Erosion calderas: Origins, processes, structural and climatic control: Bulletin of Volcanology, v. 61, p. 174–193.

Kochel, R.C., and Baker, V.R., 1990, Groundwater sapping and the geomorphic development of large Hawaiian valleys, *in* Higgins, C.G., and Coates, D.R., eds., Groundwater Geomorphology: The Role of Subsurface Water in Earth-Surface Processes and Landforms: Geological Society of America Special Paper 252, p. 245–257.

Kochel, R.C., and Piper, J.F., 1986, Morphology of large valleys on Hawai'i—Evidence for groundwater sapping and comparisons with Martian valleys: Journal of Geophysical Research–Solid Earth and Planets, v. 91, no. B13, p. E175–E192.

Laity, J.E., and Malin, M.C., 1985, Sapping processes and the development of theater-headed valley networks on the Colorado Plateau: Geological Society of America Bulletin, v. 96, p. 203–217, doi: 10.1130/0016-7606(1985)96<203:SPATDO>2.0.CO;2.

Lamb, M.P., Howard, A.D., Johnson, J., Whipple, K.X., Dietrich, W.E., and Perron, J.T., 2006, Can springs cut canyons into rock?: Journal of Geophysical Research, v. 111, no. E07002, doi: 10.1029/2005JE002663.

Ludwig, K., Szabo, B., Moore, J., and Simmons, K., 1991, Crustal subsidence rates off Hawai'i determined from $^{234}U/^{238}U$ ages of drowned coral reefs: Geology, v. 19, p. 171–174, doi: 10.1130/0091-7613(1991)019<0171:CSROHD>2.3.CO;2.

Macdonald, G.A., Abbott, A.T., and Peterson, F.L., 1983, Volcanoes in the Sea: The Geology of Hawai'i: Honolulu, University of Hawai'i Press, 517 p.

Malin, M.C., and Carr, M.H., 1999, Groundwater formation of Martian valleys: Nature, v. 397, no. 6720, p. 589–591, doi: 10.1038/17551.

McDougall, I., and Swanson, D.A., 1972, Potassium-argon ages of lavas from Hawi and Pololū volcanic series, Kohala Volcano, Hawai'i: Geological Society of America Bulletin, v. 83, no. 12, p. 3731–3737, doi: 10.1130/0016-7606(1972)83[3731:PAOLFT]2.0.CO;2.

McMurtry, G.M., Fryer, G.J., Tappin, D.R., Wilkinson, I.P., Williams, M., Fietzke, J., Garbe-Schoenberg, D., and Watts, P., 2004, Megatsunami deposits on Kohala Volcano, Hawai'i, from flank collapse of Mauna Loa: Geology, v. 32, no. 9, p. 741–744, doi: 10.1130/G20642.1.

Moore, J.G., and Clague, D.A., 1992, Volcano growth and evolution of the island of Hawai'i: Geological Society of America Bulletin, v. 104, no. 11, p. 1471–1484, doi: 10.1130/0016-7606(1992)104<1471:VGAEOT>2.3.CO;2.

Moore, J.G., and Fornari, D.J., 1984, Drowned reefs as indicators of the rate of subsidence of the Island of Hawai'i: The Journal of Geology, v. 92, p. 752–759.

Moore, J.G., Clague, D.A., Holcomb, R.T., Lipman, P.W., Normark, W.R., and Torresan, M.E., 1989, Prodigious submarine landslides on the Hawaiian ridge: Journal of Geophysical Research–Solid Earth and Planets, v. 94, no. B12, p. 17,465–17,484.

Moore, J.G., Normark, W.R., and Holcomb, R.T., 1994, Giant Hawaiian landslides: Annual Review of Earth and Planetary Sciences, v. 22, p. 119–144, doi: 10.1146/annurev.ea.22.050194.001003.

Nash, D.J., 1996, Groundwater sapping and valley development in the Hackness Hills, north Yorkshire, England: Earth Surface Processes and Landforms, v. 21, no. 9, p. 781–795, doi: 10.1002/(SICI)1096-9837(199609)21:9<781::AID-ESP616>3.0.CO;2-O.

Philbrick, S.S., 1974, What future for Niagara Falls?: Geological Society of America Bulletin, v. 85, no. 1, p. 91–98, doi: 10.1130/0016-7606(1974)85<91:WFFNF>2.0.CO;2.

Pieri, D., 1976, Distribution of small channels on Martian surface: Icarus, v. 27, no. 1, p. 25–50, doi: 10.1016/0019-1035(76)90182-2.

Pillans, B., 1985, Drainage initiation by subsurface flow in South Taranaki, New Zealand: Geology, v. 13, p. 262–265, doi: 10.1130/0091-7613(1985)13<262:DIBSFI>2.0.CO;2.

Rosenbloom, N.A., and Anderson, R.S., 1994, Hillslope and channel evolution in a marine terraced landscape, Santa Cruz, California: Journal of Geophysical Research, v. 99, no. B7, p. 14,013–14,029, doi: 10.1029/94JB00048.

Satake, K., and Smith, J.R., 2000, Tsunami modeling from Hawaiian submarine landslides. Eos (Transactions, American Geophysical Union), v. 81, p. WP251.

Schmeeckle, M.W., Nelson, J.M., Pitlick, J., and Bennett, J.P., 2001, Interparticle collision of natural sediment

grains in water: Water Resources Research, v. 37, no. 9, p. 2377–2391, doi: 10.1029/2001WR000531.

Schumm, S.A., Boyd, K.F., Wolff, C.G., and Spitz, W.J., 1995, A ground-water sapping landscape in the Florida Panhandle: Geomorphology, v. 12, no. 4, p. 281–297, doi: 10.1016/0169-555X(95)00011-S.

Scott, G.A.J., and Street, J.M., 1976, The role of chemical weathering in the formation of Hawaiian amphitheatre-headed valleys: Zeitschrift für Geomorphologie, v. 20, p. 171–189.

Seidl, M.A., Dietrich, W.E., and Kirchner, J.W., 1994, Longitudinal profile development into bedrock: An analysis of Hawaiian channels: The Journal of Geology, v. 102, p. 457–474.

Seidl, M.A., Weissel, J.K., and Pratson, L.F., 1996, The kinematics and pattern of escarpment retreat across the rifted continental margin of SE Australia: Basin Research, v. 8, no. 3, p. 301–316, doi: 10.1046/j.1365-2117.1996.00266.x.

Seidl, M.A., Finkel, R.C., Caffee, M.W., Hudson, G.B., and Dietrich, W.E., 1997, Cosmogenic isotope analysis applied to river longitudinal profile evolution: Problems and interpretations: Earth Surface Processes and Landforms, v. 22, p. 195–209, doi: 10.1002/(SICI)1096-9837(199703)22:3<195::AID-ESP748>3.0.CO;2-0.

Selby, M.J., 1993, Hillslope Materials and Processes: Oxford, Oxford University Press, 451 p.

Sklar, L.S., and Dietrich, W.E., 2001, Sediment and rock strength controls on river incision into bedrock: Geology, v. 29, no. 12, p. 1087–1090, doi: 10.1130/0091-7613(2001)029<1087:SARSCO>2.0.CO;2.

Sklar, L.S., and Dietrich, W.E., 2004, A mechanistic model for river incision into bedrock by saltating bed load: Water Resources Research, v. 40, no. 6, article no. W06301.

Sklar, L.S., and Dietrich, W.E., 2006, The role of sediment in controlling steady-state bedrock channel slope: Implications of the saltation-abrasion incision model: Geomorphology, v. 82, p. 58–83.

Smith, J.R., Satake, K., Morgan, J.K., and Lipman, P.W., 2002, Submarine landslides and volcanic features on Kohala and Mauna Kea Volcanoes and the Hana Ridge, Hawai'i, *in* Takanashi, E., Lipman, P.W., Garcia, M.O., Naka, J., and Aramaki, S., eds., Hawaiian Volcanoes: Deep Underwater Perspectives: American Geophysical Union Geophysical Monograph 128, p. 11–28.

Squyres, S.W., 1989, Urey Prize Lecture—Water on Mars: Icarus, v. 79, no. 2, p. 229–288, doi: 10.1016/0019-1035(89)90078-X.

Stearns, H.T., 1985, Geology of the State of Hawai'i: Palo Alto, California, Pacific Books, 266 p.

Stearns, H.T., and MacDonald, G.A., 1946, Geology and ground-water resources of the island of Hawai'i: Hawai'i Division of Hydrography Bulletin: Honolulu, Advertiser Publishing Co., 430 p.

Stearns, H.T., and Vaksvik, K.N., 1935, Geology and ground-water resources of the island of Oahu, Hawai'i: Hawai'i Division of Hydrography Bulletin: Wailuku, Maui Publishing Company, 536 p.

Szabo, B., and Moore, J.G., 1986, Age of –360 m reef terrace, Hawai'i, and the rate of late Pleistocene subsidence of the island: Geology, v. 14, p. 967–968, doi: 10.1130/0091-7613(1986)14<967:AOMRTH>2.0.CO;2.

Uchupi, E., and Oldale, R.N., 1994, Sapping origin of the enigmatic relict valleys of Cape Cod and Martha's Vineyard and Nantucket Islands, Massachusetts: Geomorphology, v. 9, no. 2, p. 83–95, doi: 10.1016/0169-555X(94)90068-X.

Weissel, J.K., and Seidl, M.A., 1997, Influence of rock strength properties on escarpment retreat across passive continental margins: Geology, v. 25, no. 7, p. 631–634, doi: 10.1130/0091-7613(1997)025<0631:IORSPO>2.3.CO;2.

Wentworth, C.K., 1928, Principles of stream erosion in Hawai'i: The Journal of Geology, v. 36, p. 385–410.

Wentworth, C.K., 1943, Soil avalanches on Oahu, Hawai'i: Geological Society of America Bulletin, v. 54, p. 53–64.

Whipple, K.X., 2004, Bedrock rivers and the geomorphology of active orogens: Annual Review of Earth and Planetary Sciences, v. 32, p. 151–185, doi: 10.1146/annurev.earth.32.101802.120356.

Whipple, K.X., and Tucker, G.E., 1999, Dynamics of the stream-power river incision model: Implications for height limits of mountain ranges, landscape response timescales, and research needs: Journal of Geophysical Research–Solid Earth, v. 104, no. B8, p. 17,661–17,674, doi: 10.1029/1999JB900120.

Whipple, K.X., Hancock, G.S., and Anderson, R.S., 2000, River incision into bedrock: Mechanics and relative efficacy of plucking, abrasion, and cavitation: Geological Society of America Bulletin, v. 112, no. 3, p. 490–503, doi: 10.1130/0016-7606(2000)112<0490:RIIBMA>2.3.CO;2.

White, S.F., 1949, Process of erosion on steep slopes of Oahu, Hawai'i: American Journal of Science, v. 247, p. 168–186.

Wolfe, E. W., and Morris, J., 1996, Geologic map of the Island of Hawai'i: U.S. Geological Survey Geologic Investigations Series Map I-2534-A, scale 1:1,000,000.

Yoshida, M., and Ikeda, H., 1999, The origin of the Ryumon Falls in Karasuyama Town, Tochigi Prefecture: Bulletin of the Environmental Research Center, University of Tsukuba, v. 24, p. 73–79.

Young, R., 1985, Waterfalls: Form and process: Zeitschrift für Geomorphologie, v. NF, suppl. Bd. 55, p. 81–95.

Manuscript Received 9 February 2006
Revised Manuscript Received 4 January 2007
Manuscript Accepted 19 January 2007

Printed in the USA